Electroweak baryogenesis and dark matter in a minimal extension of the MSSM

A. Menon,[1,2] D. E. Morrissey,[1,2] and C. E. M. Wagner[1,2]
[1]*HEP Division, Argonne National Laboratory, 9700 Cass Ave., Argonne, Illinois 60439, USA*
[2]*Enrico Fermi Institute, Univ. of Chicago, 5640 S. Ellis Ave., Chicago, Illinois 60637, USA*
(Received 7 May 2004; published 19 August 2004)

We examine the possibility of electroweak baryogenesis and dark matter in the nMSSM, a minimal extension of the MSSM with a singlet field. This extension avoids the usual domain wall problem of the NMSSM, and also appears as the low energy theory in models of dynamical electroweak symmetry breaking with a so-called fat-Higgs boson. We demonstrate that a strong, first order electroweak phase transition, necessary for electroweak baryogenesis, may arise in regions of parameter space where the lightest neutralino provides an acceptable dark matter candidate. We investigate the parameter space in which these two properties are fulfilled and discuss the resulting phenomenology. In particular, we show that there are always two light *CP*-even and one light *CP*-odd Higgs bosons with masses smaller than about 250 GeV. Moreover, in order to obtain a realistic relic density, the lightest neutralino mass tends to be smaller than $M_Z/2$, in which case the lightest Higgs boson decays predominantly into neutralinos.

DOI: 10.1103/PhysRevD.70.035005 PACS number(s): 12.60.Jv, 14.80.Cp, 14.80.Ly, 95.35.+d

I. INTRODUCTION

The standard model (SM) provides an excellent description of all elementary particle interactions up to energies of order 100 GeV. However, there are several reasons to expect that an extension of the standard model description is needed at energies slightly above this scale. The most important of these is the precise mechanism for the generation of elementary particle masses. In the standard model, the Higgs mechanism provides a self-consistent parametrization of this mechanism, but relies on mass parameters that are sensitive to ultraviolet scales at the quantum level. Two ways to avoid this problem are to invoke supersymmetry, or to break the electroweak symmetry dynamically. In both cases, the new physics provides an effective energy cutoff for the SM description that is of order of the weak scale. While the construction of supersymmetric extensions consistent with low energy observables is a relatively simple task [1,2], this is much more difficult to do in models that break the electroweak symmetry dynamically due to the non-perturbative nature of the interactions in the symmetry breaking sector [3].

The standard model description also fails to answer two of the most important questions at the interface of particle physics and cosmology: the nature of the dark matter and the origin of the baryon asymmetry. A consistent dark matter density may easily arise in the presence of stable, neutral, weakly interacting particles with masses of order of the weak scale. In this sense, the observation of a nonvanishing dark matter density provides an additional motivation for the existence of new physics at the weak scale. The lightest supersymmetric particle (LSP) in models of low-energy supersymmetry with R-parity conservation provides a natural source for the observed dark-matter density [1,2].

There are several ways of explaining the origin of the matter-antimatter asymmetry. Some of them rely on physics at scales much larger than the weak scale. Leptogenesis, for instance, provides a mechanism for the generation of a lepton asymmetry via the decay of heavy Majorana neutrinos which explains the smallness of the neutrino masses in the see-saw framework. This lepton asymmetry is subsequently transformed into a baryon asymmetry via anomalous weak interaction processes: baryogenesis proceeds from leptogenesis [4,5]. Due to the high-energy nature of the fundamental interactions leading to leptogenesis, it is difficult to test the realization of this scenario by weak-scale experiments.

Electroweak baryogenesis [6] provides an alternative to models of baryogenesis at high-energies, relying only on physics at the weak scale. The realization of this scenario demands that the anomalous baryon-number violating processes are out of equilibrium in the broken phase at the critical temperature of the electroweak symmetry breaking phase transition. This is possible only if the phase transition is strongly first order, or equivalently,

$$\frac{\varphi(T_c)}{T_c} \gtrsim 1, \tag{1}$$

where $\varphi(T_c)$ is the Higgs vacuum expectation value in the broken phase at the critical temperature T_c. Such a strongly first order transition cannot be achieved within the SM framework.

Supersymmetric theories introduce new physics at the weak scale which may lead to a sufficiently strong first order phase transition. This can be achieved even within the minimal supersymmetric extension of the SM (MSSM). However, in the minimal case, this demands Higgs boson masses only slightly above the present experimental bounds and a light stop with a mass below that of the top-quark [7]. Therefore, this scenario is highly constrained and may be soon tested by the Tevatron collider experiments [8].

As we will explain in the next section, there are good reasons to go beyond the minimal supersymmetric framework. In this work we shall study a minimal extension of the MSSM which includes a singlet field having restricted interactions. In Sec. II, after motivating this extension, we will describe its most relevant properties. In Sec. III we will define the model precisely, set out our notation, and study the

TABLE I. Charges of fields under the Abelian symmetries discussed in the text.

	$\hat{H}_1$	$\hat{H}_2$	$\hat{S}$	$\hat{Q}$	$\hat{L}$	$\hat{U}^c$	$\hat{D}^c$	$\hat{E}^c$	W
$U(1)_Y$	$-1/2$	$1/2$	0	$1/6$	$-1/2$	$-2/3$	$1/3$	1	0
$\mathbb{Z}_3 \subset U(1)_{PQ}$	1	1	-2	-1	-1	0	0	0	0
$U(1)_R$	0	0	2	1	1	1	1	1	2
$\mathbb{Z}_5^R, \mathbb{Z}_7^R \subset U(1)_{R'}$	1	1	4	2	2	3	3	3	6

particle spectrum at zero-temperature as well as the collider constraints. Section IV consists of an investigation of the strength of the electroweak phase transition within the nMSSM. In Sec. V we will study some of the cosmological implications of the model. In particular, we will investigate the constraints on the model that arise if it is to provide a realistic dark matter density. Section VI consists of a discussion of the resulting phenomenology based on the results of the previous sections. We reserve Sec. VII for our conclusions.

II. MINIMAL EXTENSION OF THE MSSM WITH A SINGLET SUPERFIELD

The minimal supersymmetric extension of the SM stabilizes the gauge hierarchy, leads naturally to a consistent unification of the gauge couplings near the Planck scale, and provides a viable dark matter candidate if the neutralino, a superpartner of the neutral Higgs and gauge boson particles, is the LSP [1,2]. Despite these successes, the model has some unattractive features as well, among which is the μ-problem. Namely, the μ term, $\mu \hat{H}_1 \cdot \hat{H}_2$, must be included in the superpotential, with $|\mu|$ of order of the weak scale, if the electroweak symmetry is to be broken. While the μ parameter is stable under quantum corrections as a result of supersymmetry, it is difficult (although possible [9]) to explain why this dimensional quantity should be so much smaller than M_P or M_{GUT}.

A simple solution is to replace μ by the VEV of a gauge singlet chiral superfield, $\hat{S}$. Other dimensional couplings involving the singlet are then forbidden by demanding that the superpotential obey an additional symmetry. In the most common formulation, the next-to-minimal supersymmetric SM (NMSSM) [10], one imposes a $\mathbb{Z}_3$ symmetry under which the fields transform as $\hat{\Phi}_i \to \exp(2\pi i q_i/3)\hat{\Phi}_i$, where the charges q_i are given in Table I. The most general renormalizable superpotential is then

$$W_{ren} = \lambda \hat{S} \hat{H}_1 \cdot \hat{H}_2 + \kappa \hat{S}^3 + y_u \hat{Q} \cdot \hat{H}_2 \hat{U}^c + y_d \hat{Q} \cdot \hat{H}_1 \hat{D}^c + y_e \hat{L} \cdot \hat{H}_1 \hat{E}^c, \quad (2)$$

where $\hat{S}$ is the singlet superfield and the other fields are the same as in the MSSM. Except for the cubic singlet self-coupling, this is just the MSSM superpotential with a field dependent μ-term proportional to the singlet field. Without this additional cubic term, the superpotential is invariant under an anomalous $U(1)_{PQ}$, whose charges are listed in Table I, that gives rise to an unacceptable axion [11]. The cubic term explicitly breaks $U(1)_{PQ}$ down to its maximal $\mathbb{Z}_3$ subgroup, thereby removing the axion while still forbidding all dimensionful couplings. Unfortunately, this generates new difficulties. When the singlet acquires a VEV, necessarily near the electroweak scale, the $\mathbb{Z}_3$ symmetry is broken as well producing cosmologically unacceptable domain walls [12]. The domain wall problem can be avoided if $\mathbb{Z}_3$ violating non-renormalizable operators are included. However, such operators generate a large singlet tadpole that destabilizes the hierarchy [13].

As shown in [14–16], both problems can be avoided in the context of an N=1 supergravity scenario. In the absence of the cubic singlet term, the superpotential of Eq. (2) obeys the $U(1)_{PQ}$, and $U(1)_R$ symmetries listed in Table I, and so is also invariant under the group $U(1)_{R'}$ with charges $R' = 3R + PQ$. This symmetry alone is enough to give the superpotential of Eq. (2) with no cubic term, as are the maximal $\mathbb{Z}_5^R$ and $\mathbb{Z}_7^R$ subgroups of $U(1)_{R'}$. If we now demand that both the superpotential and the Kähler potential obey one of these discrete R-symmetries instead of the $\mathbb{Z}_3$ symmetry of the NMSSM, the superpotential will be of the desired form up to a possible singlet tadpole term. Using power counting arguments it may be shown that a singlet tadpole does arise, but only at the six ($\mathbb{Z}_5^R$) or seven ($\mathbb{Z}_5^R$) loop level. The loop suppression in both cases is large enough that the induced tadpole does not destabilize the hierarchy [14,15]. Therefore, this mechanism very elegantly solves three problems: it prevents the appearance of dimensional couplings (other than the tadpole) in the renormalizable part of the superpotential; the induced singlet tadpole explicitly breaks $U(1)_{PQ}$ and its discrete subgroups, thereby avoiding unacceptable axions and domain walls; and the loop suppression of the tadpole leads naturally to a singlet VEV of the order of M_{SUSY}. Following [16], we shall refer to this model as the nearly minimal supersymmetric standard model (nMSSM).

Another interesting feature of the model is that something like R-parity arises from the imposed R-symmetries. These symmetries forbid the appearance of all $d=4$ B- and L-violating operators as well as the dominant higher dimensional B-violating operators that contribute to proton decay. While proton stability is ensured, there are non-renormalizable operators that make the LSP unstable. As will be shown in Sec. III A, the LSP of the model under study is nearly always the lightest neutralino. In the $\mathbb{Z}_7^R$ symmetric case, this symmetry forbids all $d \leqslant 6$ operators that could lead to the decay of such an LSP, and naïve dimensional analysis shows that it has a lifetime in excess of the age of the Universe. The issue is a bit more delicate in the $\mathbb{Z}_5^R$ case since the L-violating $d=5$ operator $\hat{S}\hat{S}\hat{H}_2\hat{L}$ is allowed by the symmetry. We find that the lifetime of the neutralino LSP induced by this operator is greater than the age of the Universe provided the cutoff scale (by which non-renormalizable operators are suppressed) exceeds $\Lambda \gtrsim 3 \times 10^{14}$ GeV. The details of our estimate are presented in Appendix B. Therefore, the same symmetries that ensure a

natural solution to the μ-problem stabilize the LSP, and provide the means for a sufficiently large proton lifetime.

The nMSSM is quite attractive for a number of phenomenological reasons as well. In the MSSM, large stop masses, high $\tan\beta$, and some fine-tuning are needed to evade the LEP-II Higgs boson mass bounds [17]. These bounds are much easier to avoid in the nMSSM and the NMSSM since there is an additional tree-level contribution to the *CP*-even Higgs boson masses. The same LEP-II bounds on the lightest neutral Higgs boson also put severe constraints on the parameter space consistent with electroweak baryogenesis (EWBG) within the MSSM [18]. On the other hand, EWBG does appear to be possible within the NMSSM [19–22] and other singlet extensions [23] due to additional terms in the tree-level potential. We find that the same holds true for the nMSSM.

Finally, we note that the superpotential and soft-breaking terms of the nMSSM also arise as the low-energy effective theory of minimal supersymmetric models with dynamical electroweak symmetry breaking, the so-called ''Fat-Higgs'' models [24]. In these models, the value of the Higgs-singlet coupling λ is not restricted by the requirement of perturbative consistency up to the grand-unification scale. Instead, the precise value of λ depends on the scale of dynamical symmetry breaking, λ being larger for smaller values of this scale. In our work, we shall focus on the case where perturbative consistency holds up to high-energy scales, but we will also comment on how our results are modified if we ignore the perturbativity constraint on λ.

III. THE NMSSM AT ZERO TEMPERATURE

Much of the analysis and notation in this section follows that of [15]. For simplicity, we will include only the Higgs, singlet, and third generation quark-squark fields in the superpotential. The superpotential, including the loop-generated tadpole term, is then

$$W_{nMSSM}=\lambda\hat{S}\hat{H}_1\cdot\hat{H}_2+\frac{m_{12}^2}{\lambda}\hat{S}+y_t\hat{Q}\cdot\hat{H}_2\hat{U}^c+\cdots \tag{3}$$

where $\hat{H}_1^t=(\hat{H}_1^0,\hat{H}_1^-)$, $\hat{H}_2^t=(\hat{H}_2^+,\hat{H}_2^0)$ denote the two Higgs superfields, $\hat{S}$ is the singlet superfield, and $A\cdot B=\epsilon^{ab}A_aB_b$ with $\epsilon^{12}=1$.

The tree-level potential is then $V_0=V_F+V_D+V_{soft}$:

$$\begin{aligned}V_F=&\left|\lambda H_1\cdot H_2+\frac{m_{12}^2}{\lambda}\right|^2+|\lambda SH_1^0+y_t\tilde{t}_L\tilde{t}_R^*|^2\\&+|\lambda SH_1^-+y_t\tilde{b}_L\tilde{t}_R^*|^2+|\lambda S|^2H_2^\dagger H_2\\&+|y_t\tilde{t}_R^*|^2H_2^\dagger H_2+|y_t\tilde{Q}\cdot H_2|^2,\end{aligned}$$

$$V_D=\frac{\overline{g^2}}{8}(H_2^\dagger H_2-H_1^\dagger H_1)^2+\frac{g^2}{2}|H_1^\dagger H_2|^2, \tag{4}$$

$$\begin{aligned}V_{soft}=&m_1^2H_1^\dagger H_1+m_2^2H_2^\dagger H_2+m_s^2|S|^2+(t_sS+\text{H.c.})\\&+(a_\lambda SH_1\cdot H_2+\text{H.c.})+m_Q^2\tilde{Q}^\dagger\tilde{Q}+m_U^2|\tilde{t}_R|^2\\&+(a_t\tilde{Q}\cdot H_2\tilde{t}_R^*+\text{H.c.}).\end{aligned}$$

In writing V_D we have defined $\overline{g}=\sqrt{g^2+g'^2}=g/\cos\theta_W$.

The couplings $a_\lambda, t_s, \lambda, m_{12}^2, y_t, a_t$ can all be complex, but not all their phases are physical. By suitable redefinitions of $\hat{S},\hat{H}_1$, and $\hat{H}_2$, the parameters λ and m_{12}^2 can both be made real [25]. To simplify the analysis and to avoid spontaneous *CP* violation, we shall assume that the soft-breaking parameters a_λ, t_s, a_t and the Yukawa y_t are also real.[1] Moreover, we may take a_λ and t_s to be positive provided we allow λ and m_{12}^2 to have either sign. Real parameters are not sufficient to exclude spontaneous *CP* violation, however, so we must check this explicitly. We must also verify that the potential does not generate a VEV for either of the charged Higgs fields.

If none of the squark fields get VEV's, the tree-level Higgs potential becomes

$$\begin{aligned}V_0=&m_1^2H_1^\dagger H_1+m_2^2H_2^\dagger H_2+m_s^2|S|^2+\lambda^2|H_1\cdot H_2|^2\\&+\lambda^2|S|^2(H_1^\dagger H_1+H_2^\dagger H_2)+\frac{\overline{g^2}}{8}(H_2^\dagger H_2-H_1^\dagger H_1)^2\\&+\frac{g^2}{2}|H_1^\dagger H_2|^2+t_s(S+\text{H.c.})+a_\lambda(SH_1\cdot H_2+\text{H.c.})\\&+m_{12}^2(H_1\cdot H_2+\text{H.c.}).\end{aligned} \tag{5}$$

We may choose an $SU(2)\times U(1)$ gauge such that $\langle H_1^-\rangle=0$ and $\langle H_1^0\rangle\in\mathbb{R}^{\geqslant}$ at the minimum of the potential. Taking the derivative of V_0 with respect to H_2^+ and evaluating the result at the minimum, we find

$$\begin{aligned}\frac{\partial V_0}{\partial H_2^+}\Big|_{H_i=v_i}=v_+^*\Bigg[&m_2^2+\lambda^2|v_s|^2+\frac{\overline{g^2}}{4}(|v_2|^2-v_1^2)\\&+\frac{g^2}{2}v_1^2+\frac{\overline{g^2}}{8}|v_+|^2\Bigg],\end{aligned} \tag{6}$$

where we have defined $\langle H_2^0\rangle=v_2$, $\langle H_2^+\rangle=v_+$, and $\langle S\rangle=v_s$. It follows that $\langle H_2^+\rangle$ vanishes at the minimum provided $m_2^2+\lambda^2|v_s|^2+(\overline{g^2}/4)(|v_2|^2-v_1^2)+(g^2/2)v_1^2>0$.

If the charged Higgs VEV's vanish at the minimum, the only part of the potential that depends on the phases of the Higgs fields are the last three terms in Eq. (5):

$$\begin{aligned}V_{phase}=&t_s(S+\text{H.c.})+a_\lambda(SH_1^0H_2^0+\text{H.c.})\\&+m_{12}^2(H_1^0H_2^0+\text{H.c.}).\end{aligned} \tag{7}$$

[1]This assumption is not completely *ad hoc*. Within a minimal supergravity scenario, the soft breaking parameters are proportional to the corresponding terms in the superpotential.

Recalling that a_λ and t_s are both real and positive, the potential will have an absolute minimum with $\langle S\rangle = v_s \in \mathbb{R}^{\leqslant}$ and $\langle H_2^0\rangle = v_2 \in \mathbb{R}^{\geqslant}$ provided $m_{12}^2 < 0$. While this condition is sufficient to avoid spontaneous *CP* violation, the result of [26] indicates that it is not necessary. We will focus on the $m_{12}^2 < 0$ case because it simplifies the analysis, and as we shall see below, is preferred by the constraints on the scalar Higgs boson masses. However, we have also examined the $m_{12}^2 > 0$ case, and find that once we impose the experimental constraints described in the following section, the parameter space with $m_{12}^2 > 0$ is very restricted, and tends to be inconsistent with electroweak baryogenesis.

With $m_{12}^2 < 0$, the field VEV's are all real and have fixed sign:

$$\langle S\rangle = v_s < 0 \quad \langle H_1^0\rangle = v_1 > 0, \quad \langle H_2^0\rangle = v_2 > 0. \tag{8}$$

We define the angle β as in the MSSM:

$$v_1 = v\cos\beta, \quad v_2 = v\sin\beta, \tag{9}$$

with $v \simeq 174$ GeV. We also define $\mu = -\lambda v_s$, since this is the quantity that corresponds to the μ parameter in the MSSM. Note that μ can have either sign, depending on the sign of λ.

The minimization conditions for H_1^0, H_2^0, and S can be used to relate the scalar soft masses to the other parameters in terms of the VEV's. These give

$$\begin{aligned}
m_1^2 &= -(m_{12}^2 + a_\lambda v_s)\frac{v_2}{v_1} - \frac{\overline{g^2}}{4}(v_1^2 - v_2^2) - \lambda^2(v_2^2 + v_s^2) \\
&\quad - \frac{1}{2v_1}\frac{\partial \Delta V}{\partial H_1^0}\bigg|_{H_1^0 = v_1}, \\
m_2^2 &= -(m_{12}^2 + a_\lambda v_s)\frac{v_1}{v_2} + \frac{\overline{g^2}}{4}(v_1^2 - v_2^2) - \lambda^2(v_1^2 + v_s^2) \\
&\quad - \frac{1}{2v_2}\frac{\partial \Delta V}{\partial H_2^0}\bigg|_{H_2^0 = v_2}, \\
m_s^2 &= -a_\lambda \frac{v_1 v_2}{v_s} - \frac{t_s}{v_s} - \lambda^2 v^2 - \frac{1}{2v_s}\frac{\partial \Delta V}{\partial S}\bigg|_{S = v_s},
\end{aligned} \tag{10}$$

where ΔV consists of contributions to the effective potential beyond tree level. To one-loop order

$$\Delta V = \frac{1}{(4\pi)^2}\left[\sum_b g_b h(m_b^2) - \sum_f g_f h(m_f^2)\right], \tag{11}$$

where the first sum runs over all bosons, the second over all Weyl fermions, g_i is the number of (on-shell) degrees of freedom, m_i is the field-dependent mass eigenvalue, and the function $h(m^2)$ is given by (in the $\overline{DR}$ scheme)

$$h(m^2) = \frac{m^4}{4}\left[\ln\left(\frac{m^2}{Q^2}\right) - \frac{3}{2}\right]. \tag{12}$$

The one-loop corrections are therefore given by

$$\begin{aligned}
\Delta m_i^2 = -\frac{2}{64\pi^2}\Bigg(&\sum_b g_b m_b^2 \frac{\partial m_b^2}{\partial H_i^2}\left[\ln\left(\frac{m_b^2}{Q^2}\right) - 1\right] \\
&- \sum_f g_f m_f^2 \frac{\partial m_f^2}{\partial H_i^2}\left[\ln\left(\frac{m_f^2}{Q^2}\right) - 1\right]\Bigg)\Bigg|_{H_i = v_i}.
\end{aligned} \tag{13}$$

A. Charginos and neutralinos

The chargino and neutralino sectors provide important phenomenological constraints on the model. The fermion component of the singlet superfield, the singlino, leads to a fifth neutralino state. Assuming the sfermions to be heavy, with masses of order a few hundred GeV, and values of λ that remain perturbative up to a grand unification scale of order 10^{16} GeV, the LSP of the model is always the lightest neutralino with a mass below about 60 GeV.

The chargino mass matrix, in the basis $(\tilde{W}^+, \tilde{H}_2^+, \tilde{W}^-, \tilde{H}_1^-)$, is

$$M_{\chi^\pm} = \begin{pmatrix} 0 & X^t \\ X & 0 \end{pmatrix}, \tag{14}$$

where

$$X = \begin{pmatrix} M_2 & \sqrt{2}s_\beta M_W \\ \sqrt{2}c_\beta M_W & -\lambda v_s \end{pmatrix}. \tag{15}$$

For the neutralinos, the mass matrix in basis $\psi_i^0 = (\tilde{B}^0, \tilde{W}^0, \tilde{H}_1^0, \tilde{H}_2^0, \tilde{S})$ reads

$$\mathcal{M}_{\tilde{N}} = \begin{pmatrix} M_1 & \cdot & \cdot & \cdot & \cdot \\ 0 & M_2 & \cdot & \cdot & \cdot \\ -c_\beta s_w M_Z & c_\beta c_w M_Z & 0 & \cdot & \cdot \\ s_\beta s_w M_Z & -s_\beta c_w M_Z & \lambda v_s & 0 & \cdot \\ 0 & 0 & \lambda v_2 & \lambda v_1 & 0 \end{pmatrix}. \tag{16}$$

In our analysis we take $M_1 = (\alpha_1/\alpha_2)M_2 \simeq \frac{1}{2}M_2$, which corresponds to what would be expected from universality at the GUT scale. With an eye towards electroweak baryogenesis, we allow the gaugino masses to have a common phase: $M_2 = Me^{i\phi}$ with M real. This phase also has a significant effect on the mass of the lightest neutralino. Since flipping the sign of λ is equivalent to shifting the gaugino phase by $\phi \to \phi + \pi$, we will consider only the $\lambda > 0$ case.

To see how the light neutralino state arises, suppose M_1 and M_2 are very large and real so that the gaugino states decouple, leaving only the lower 3×3 Higgsino block. For $v_1 \ll v_2, v_s$, the smallest eigenvalue of this matrix is then

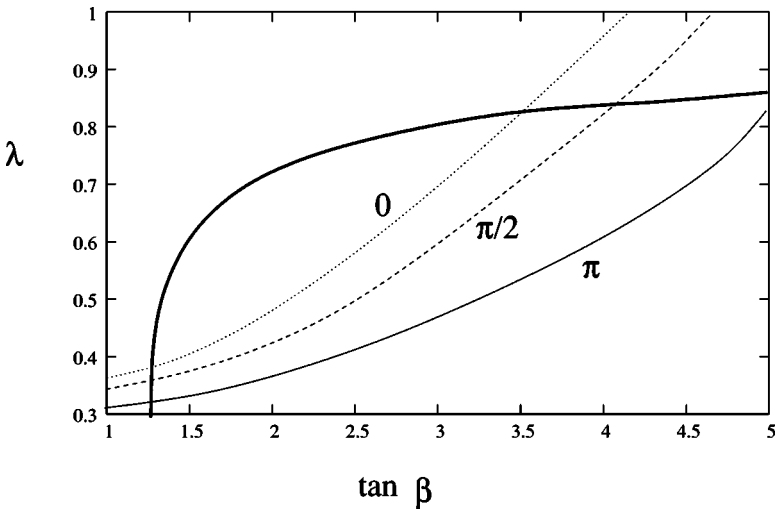

FIG. 1. Allowed regions in the tan β-λ plane. The region consistent with perturbative unification lies below the thick solid line, while the regions consistent with the LEP II constraints (and $m_{\tilde{N}_1} > 25$ GeV) lie above the thinner lines. Among these, the solid line corresponds to a gaugino phase of $\phi = \pi$, while the dotted and dashed lines correspond to $\phi = 0$, $\pi/2$ respectively.

$$m_{\tilde{N}_1} \simeq 2\lambda v_1 v_2 v_s/(v_1^2+v_2^2+v_s^2), \tag{17}$$

and the corresponding state is predominantly singlino. More generally, the mass eigenstates are

$$\tilde{N}_i = N_{ij}\psi_j^0, \tag{18}$$

where N_{ij} is a unitary matrix such that $N^* \mathcal{M}_{\tilde{N}} N^\dagger$ is diagonal with non-negative entries [1]. We label the states in order of increasing mass so that $\tilde{N}_1$ is the lightest neutralino.

Measurements made at LEP II impose stringent constraints on the chargino-neutralino spectrum. Since the coupling of the charginos to gauge bosons is the same as in the MSSM, the mass of the lightest chargino must satisfy $m_{\chi_1^\pm} > 104$ GeV [27]. The corresponding requirement for the neutralinos is either $(m_{\tilde{N}_1} + m_{\tilde{N}_2}) > 209$ GeV, or $\sigma(e^+e^- \to \tilde{N}_1\tilde{N}_2) \lesssim 10^{-2}$ fb. Finally, for $m_{\tilde{N}_1} < M_Z/2$, we must have $BR(Z \to \tilde{N}_1\tilde{N}_1) < 0.8 \times 10^{-3}$ [28].

It is possible to satisfy all of these constraints in the limit of large tan β, in which case $\tilde{N}_1$ is a very light LSP; $m_{\tilde{N}_1} \lesssim 15$ GeV for $\lambda < 1.0$, tan $\beta > 10$, and $M_2 \to \infty$. This state is mostly singlino, and couples only weakly to the gauge bosons. However, this limit also leads to an unacceptably large neutralino relic density. As we will show in Sec. V, for heavy sfermions, the dominant annihilation channel for $\tilde{N}_1$ is s-channel Z-exchange.[2] For such a light, mostly singlino $\tilde{N}_1$, the $Z\tilde{N}_1\tilde{N}_1$ coupling is too weak for this state to annihilate efficiently.

We are thus led to consider values of tan β of order unity. The $\tilde{N}_1$ state now has a sizeable Higgsino component and correspondingly large couplings to the gauge bosons, so there is a danger of producing too large a contribution to the Z-width. The branching ratio of the Z to two $\tilde{N}_1$'s is given by

$$BR(Z \to \tilde{N}_1\tilde{N}_1) = \frac{g^2}{4\pi} \frac{(|N_{13}|^2 - |N_{14}|^2)^2}{24\cos^2_W} \frac{M_Z}{\Gamma_Z}\left[1 - \left(\frac{2m_{\tilde{N}_1}}{M_Z}\right)^2\right]^{3/2}. \tag{19}$$

Combining the branching ratio constraint with that for the relic density, we find $m_{\tilde{N}_1} \gtrsim 35$ GeV is needed if both conditions are to be met. (See Sec. V.) As this value depends somewhat on parameters in the Higgs sector, we impose the weaker constraint $m_{\tilde{N}_1} > 25$ GeV in our analysis.

The magnitude of λ must be fairly large, $\lambda \gtrsim 0.3$, to raise the mass of the lightest neutralino above 25 GeV. ($|\lambda| \gtrsim 0.5$ for $m_{\tilde{N}_1} > 35$ GeV.) On the other hand, if λ is too large it encounters a Landau pole before the GUT scale. This is precisely what happens in the recently proposed fat Higgs model [24], in which the Landau pole corresponds to the Higgs compositeness scale. We would like to maintain the property of perturbative unification in the model (in the usual sense), so we will focus most of our attention on values of λ that remain perturbative up to $M_{GUT} \sim 10^{16}$ GeV. However, with the fat Higgs model in mind, we will also consider larger values of λ.

It is straightforward to derive the limit on λ at one-loop order. The relevant (one-loop) beta functions are [15]

$$\frac{dg_s}{dt} = -\frac{1}{(4\pi)^2}\frac{3}{2}g_s^3,$$

$$\frac{dy_t}{dt} = \frac{y_t}{(4\pi)^2}\left(3y_t^2 + \frac{1}{2}\lambda^2 - \frac{8}{3}g_s^2\right),$$

$$\frac{d\lambda}{dt} = \frac{\lambda}{(4\pi)^2}\left(2\lambda^2 + \frac{3}{2}y_t^2\right), \tag{20}$$

where $t = \ln(Q^2/M_Z^2)$. Running these up to $Q^2 = (10^{16}\ \text{GeV})^2$ and demanding $\lambda^2 < 4\pi$, we find the allowed region in the

[2]There are also contributions to the annihilation cross section from s-channel Higgs exchange, but these processes alone are not strong enough to produce an acceptable neutralino relic density unless the neutralino mass is close to a half of one of the Higgs boson masses.

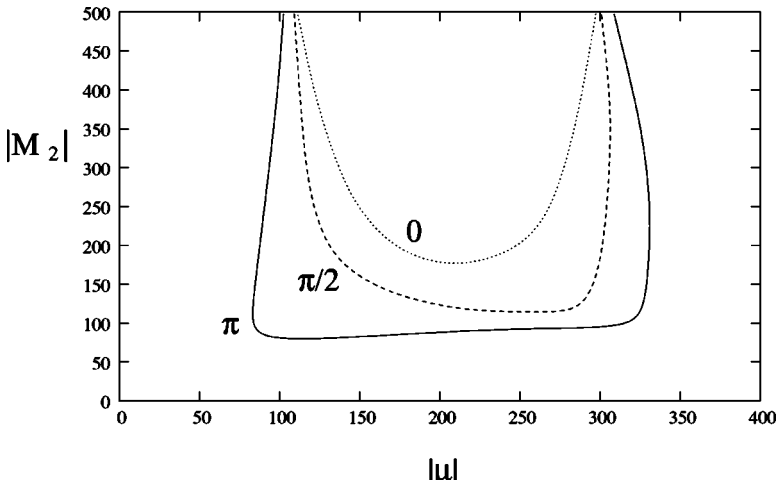

FIG. 2. Allowed regions in the $|\mu|-|M_2|$ plane for a gaugino phase of $\phi=0$, $\pi/2$, π, and $(\tan\beta,\lambda)$ below the perturbativity bound. The allowed region lies in the central area. Recall that $\mu=-\lambda v_s$ in the model.

$\tan\beta$-λ plane shown in Fig. 1. The lower limit on $\tan\beta$ comes about because small values of this quantity imply a large $y_t(m_t)$, and this accelerates the running of λ. The figure also shows the region in which the $\tilde{N}_1$ state has a mass greater than 25 GeV and satisfies the LEP II constraints listed above.

Figure 2 shows the corresponding allowed region in the $|\mu|-|M_2|$ plane. The lower bounds on $|M_2|$ and $|\mu|$ are due to the chargino mass constraint. Interestingly, there is also an upper bound on $|\mu|$, which comes from the lower bound on the lightest neutralino mass. From Eqs. (16), (17) we see that for $|v_s|\gg v$, the predominantly singlino state becomes very light. Since $\mu=-\lambda v_s$ and λ is bounded above by the perturbativity constraint, this translates into an upper bound on $|\mu|$. Both the phase and the magnitude of the gaugino mass M_2 have a significant impact on the mass of the light singlino state. The largest masses are obtained for $\phi=\pi$ with $|M_2|\sim\lambda v$, as this maximizes the constructive interference between the gaugino and Higgsino components. When $\phi=0$ the interference is destructive, and $|M_2|\to\infty$ maximizes the mass.

Figure 3 shows the range of masses of the lightest neutralino that are consistent with the constraints listed above. (The relevant input parameter sets are those listed in Table II.) For $\tan\beta$ and λ below the perturbative bound we see that the $\tilde{N}_1$ state has a mass below about 60 GeV, making it the LSP in the absence of a light gravitino. For $m_{\tilde{N}}$ below 50 GeV, this state is predominantly singlino, with a sizeable Higgsino component. This is because, with the assumption of gaugino mass universality, the constraint on the chargino mass puts a lower bound on $|M_1|$ that excludes a lighter predominantly *B*-ino state. However, a mostly *B*-ino LSP is possible if the light singlino state has a mass above about 50 GeV, although the parameter space in which this can occur, consistent with perturbative unification, is severely restricted. In this event, the LSP and NLSP must be very close in mass. If λ is allowed to exceed the perturbativity bound, the situation is much less constrained; the parameter space in which the LSP is mostly *B*-ino becomes much larger, and a *B*-ino LSP need no longer be nearly degenerate with the NLSP.

B. Higgs spectrum

The LEP II lower bound on the mass of the lightest neutral *CP*-even Higgs boson of about 114 GeV is difficult to evade in the MSSM. This follows from the fact that, at tree level, the mass of this state is bounded by M_Z,

$$m_h^2\leq M_Z^2\cos^2 2\beta, \tag{21}$$

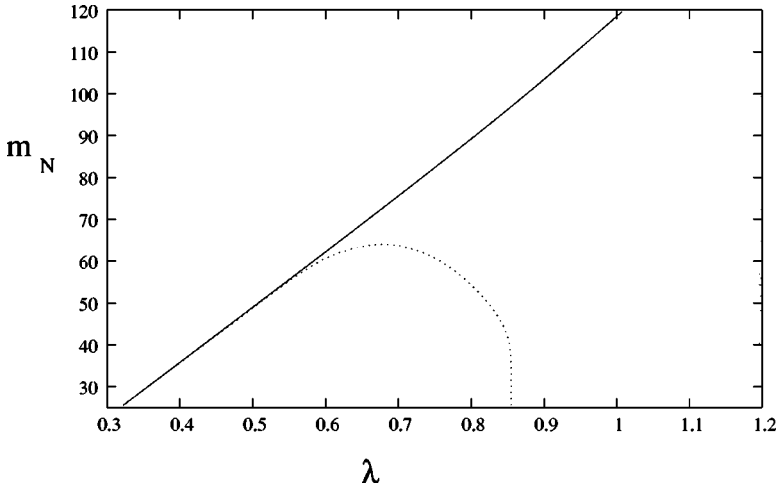

FIG. 3. Mass of the lightest neutralino. The region to the right of the solid line is consistent with the LEP II constraints listed above. The region surrounded by the dotted line is also consistent with perturbative unification.

TABLE II. Ranges of input parameters.

	$\tan\beta$	λ	v_s (GeV)	a_λ (GeV)	$t_s^{1/3}$ (GeV)	M_a (GeV)	$\lvert M_2\rvert$ (GeV)	ϕ
Range	1–5	0.3–2.0	-750–0	0–1000	0–1000	200–1000	0–1000	$0-\pi$

which implies that large one-loop corrections are needed to increase the mass. The dominant loop contribution comes from the stops. With $\tan\beta \gg 1$, stop masses of order 1 TeV, and considerable fine-tuning of the stop mixing parameters, the mass of the lightest Higgs boson can be brought up to $m_h \simeq 130$ GeV [17].

The corresponding tree-level bound in the nMSSM is [16]

$$m_h^2 \leqslant M_Z^2\left(\cos^2 2\beta + \frac{2\lambda^2}{g^2}\sin^2 2\beta\right), \tag{22}$$

which exceeds 100 GeV for $|\lambda| \sim 0.7$ and $\tan\beta \sim 2$. The same bound applies in the NMSSM [29]. This makes it possible to avoid the LEP II constraint without fine-tuning in the stop sector.

In order to discuss some of the constraints on the parameter space from the Higgs sector, we list here the tree-level Higgs boson masses. We have also included the one-loop mass corrections from the top and the stops given in [15] in our numerical analysis.

Since the tree-level Higgs VEV's are real, and neglecting the small *CP*-violating effects associated with the one-loop chargino and neutralino contributions [30], the Higgs fields can be expanded as

$$H_1 = \begin{pmatrix} v_1 + \frac{1}{\sqrt{2}}(\phi_1 + i a_1) \\ \phi_1^- \end{pmatrix},$$

$$H_2 = \begin{pmatrix} \phi_2^+ \\ v_2 + \frac{1}{\sqrt{2}}(\phi_2 + i a_2) \end{pmatrix},$$

$$S = v_s + \frac{1}{\sqrt{2}}(\phi_s + i a_s). \tag{23}$$

After electroweak symmetry breaking, the real and imaginary parts of the singlet mix with those of H_1^0 and H_2^0 to produce two neutral scalar states in addition to those of the MSSM. In all, the physical Higgs states consist of one charged scalar, two neutral *CP*-odd scalars, and three neutral *CP*-even scalars.

For the *CP*-odd scalars, the combination $G^0 = -a_1 c_\beta + a_2 s_\beta$ is absorbed by the Z^0 while the orthogonal linear combination $A^0 = a_1 s_\beta + a_2 c_\beta$ mixes with a_s to give two physical scalars. The mass matrix in basis (A^0, a_s) is

$$M_P^2 = \begin{pmatrix} M_a^2 & -a_\lambda v \\ -a_\lambda v & -\frac{1}{v_s}(t_s + s_\beta c_\beta a_\lambda v^2) \end{pmatrix}, \tag{24}$$

where

$$M_a^2 = -\frac{1}{s_\beta c_\beta}(m_{12}^2 + a_\lambda v_s). \tag{25}$$

Note that Eq. (10) implies $m_s^2 + \lambda^2 v^2 = -(1/v_s)(t_s + s_\beta c_\beta a_\lambda v^2)$. Therefore the singlet soft mass, m_s^2, sets the mass scale of a predominantly singlet state.

Among the charged Higgs bosons, the combination $G^+ = \phi_2^+ s_\beta - \phi_1^{-*} c_\beta$ is taken up by the W^+ leaving behind a single complex charged scalar mass eigenstate, H^+, of mass

$$M_\pm^2 = M_a^2 + M_W^2 - \lambda^2 v^2. \tag{26}$$

It may be shown using the minimization conditions, Eq. (10), that $M_\pm^2 > 0$ is equivalent to the condition needed to avoid a charged Higgs VEV given below Eq. (6).

Finally, the mass matrix elements for the *CP*-even Higgs boson states are

$$\begin{aligned} M_{11}^2 &= s_\beta^2 M_a^2 + c_\beta^2 M_Z^2, \\ M_{12}^2 &= -s_\beta c_\beta (M_a^2 + M_Z^2 - 2\lambda^2 v^2), \\ M_{13}^2 &= v(s_\beta a_\lambda + 2 c_\beta \lambda^2 v_s), \\ M_{22}^2 &= c_\beta^2 M_a^2 + s_\beta^2 M_Z^2, \\ M_{23}^2 &= v(c_\beta a_\lambda + 2 s_\beta \lambda^2 v_s), \\ M_{33}^2 &= -\frac{1}{v_s}(t_s + s_\beta c_\beta a_\lambda v^2) = m_s^2 + \lambda^2 v^2, \end{aligned} \tag{27}$$

with the remaining elements related to these by symmetry. As for the *CP*-odd case, the mass of a mostly singlet state is determined by the singlet soft mass.

Large values of M_a^2 help to increase the mass of the Higgs states. This is most easily obtained with $m_{12}^2 < 0$ [see Eq. (25)], which is a sufficient condition to guarantee the absence of spontaneous *CP* violation at tree level. We also note that the MSSM limit of the NMSSM is not possible in this model. In this limit one takes $|v_s| \gg v$ while holding λv_s fixed, thereby decoupling the singlet states from the rest of the Higgs spectrum. As discussed in Sec. III A, such large values of v_s lead to an unacceptably light neutralino state. On the other hand, the decoupling limit of the nMSSM discussed in [15], $|t_s| \to \infty$, is still viable. Indeed, the upper

bound on the lightest neutral Higgs boson mass, Eq. (22) is saturated in this limit if $M_a^2 \to \infty$ as well.

The precise LEP II bounds on the Higgs boson masses depend on the couplings of the Higgs bosons to the gauge bosons. These couplings tend to be weakened somewhat from mixing with the singlet. Let $\mathcal{O}^S$, $\mathcal{O}^P$ be the orthogonal mixing matrices relating the gauge and mass eigenstates:

$$\begin{pmatrix} S_1 \\ S_2 \\ S_3 \end{pmatrix} = \mathcal{O}^S \begin{pmatrix} \phi_1 \\ \phi_2 \\ \phi_s \end{pmatrix}; \quad \begin{pmatrix} P_1 \\ P_2 \end{pmatrix} = \mathcal{O}^P \begin{pmatrix} A^0 \\ a_s \end{pmatrix}. \tag{28}$$

We label the mass eigenstates in order of increasing mass, so that S_1 is the lightest *CP*-even state and P_1 the lightest *CP*-odd state. In terms of these mixing matrices, the *SVV*-type couplings are

$$SZZ: \frac{\overline{g}}{2} M_Z (c_\beta \mathcal{O}^S_{k1} + s_\beta \mathcal{O}^S_{k2})(Z_\mu)^2 S_k,$$

$$SWW: \frac{g}{2} M_W (c_\beta \mathcal{O}^S_{k1} + s_\beta \mathcal{O}^S_{k2})(W_\mu)^2 S_k. \tag{29}$$

Also relevant are the *SPZ*-type couplings

$$SPZ: \quad \frac{\overline{g}}{2} [\mathcal{O}^P_{\ell 1}(s_\beta \mathcal{O}^S_{k1} - c_\beta \mathcal{O}^S_{k2})] Z^\mu S_k \overleftrightarrow{\partial}_\mu P_\ell. \tag{30}$$

The couplings of the Higgs states to fermions and neutralinos are listed in Appendix C.

The LEP bound on the charged Higgs boson is given in Ref. [31]. Assuming $BR(H^+ \to \tau^+ \nu) \simeq 1$ this bound reads, approximately,

$$M_{H^\pm} > 90 \ \text{GeV}. \tag{31}$$

The bounds on the *CP*-odd Higgs bosons depend strongly on their coupling to the Z-gauge boson and the *CP*-even scalars given in Eq. (30). If the lightest *CP*-odd Higgs boson, P_1, has a large singlet component this coupling can become very small, and the bound on this particle is much weaker than the LEP bound of about 90 GeV present in the MSSM [32]. This bound may be further weakened if the decay $P_1 \to \tilde{N}_1 \tilde{N}_1$ is allowed kinematically. If so, this mode tends to dominate the decay width leading to a large fraction of invisible final states.

The same is true of the lightest *CP*-even state, S_1. The limit found in [33] depends on the strength of the *SVV* coupling relative to the corresponding standard model coupling. From Eq. (29) this relative factor is $|c_\beta \mathcal{O}^S_{11} + s_\beta \mathcal{O}^S_{12}|$, which can be considerably smaller than unity if the S_1 state has a large singlet component. Again, the limit is further weakened if the $S_1 \to \tilde{N}_1 \tilde{N}_1$ channel is open, as this tends to dominate the decay width below the gauge boson threshold. In this case, the limit on invisible decay modes found in [34] is the relevant one.

IV. ELECTROWEAK BARYOGENESIS

If electroweak baryogenesis (EWBG) is to generate the presently observed baryon asymmetry, the electroweak phase transition must be strongly first order. In the most promising MSSM scenario, this phase transition is dominated by a light, mostly right-handed stop [35]. Such a stop produces a large contribution to the cubic term in the one-loop effective potential that is responsible for making the phase transition first order. Even so, for Higgs boson masses above the LEP II bound, there is only a very small region of parameter space in which the EW phase transition is strong enough for EWBG to work [18,36].

The prospects for EWBG in the NMSSM are more promising. The NMSSM has an additional tree-level contribution to the cubic term of the effective potential. This is sufficient to make the electroweak phase transition strongly first order without relying on the contribution of a light stop [19–23]. Since the nMSSM has a similar cubic term in the tree-level potential, we expect EWBG to be possible in this model as well.

In this section we investigate the strength to the electroweak phase transition in the nMSSM in order to find out whether a strongly first order transition is possible, and if so, try to map out the relevant region of parameter space. To simplify our analysis, we neglect the contributions from sfermions other than the stops since these are generally very small. We also fix the stop SUSY-breaking parameters to be

$$m^2_{Q_3} = m^2_{U_3} = (500 \ \text{GeV})^2,$$

$$a_t = 100 \ \text{GeV}.$$

This choice of parameters leads to stops that are too heavy to have a relevant impact on the strength of the first order phase transition. We have made this choice because it allows us to emphasize the effects induced by terms in the tree-level effective potential that are not present in the MSSM. These effects turn out to be sufficient to make the phase transition strongly first order, even in the absence of light stops.

While a strongly first order electroweak phase transition is necessary for EWBG to generate the observed baryon asymmetry, based on previous analyses of the MSSM, it appears that this condition is also sufficient [37,38]. In the MSSM, the generation of baryon number proceeds from the *CP*-violating interactions of the charginos with the Higgs field. The dominant source of *CP* violation, leading to the baryon asymmetry, is proportional to the relative phase of the μ and the gaugino mass parameters, $arg(\mu M_2)$. The only difference in the model under study is that the μ parameter is replaced by the quantity $(-\lambda v_s)$, which is real, and *CP* violation is induced by the phase of the gaugino masses. Therefore, in the presence of a sufficiently strong first order phase transition, we expect a result for the baryon asymmetry generated from the chargino currents similar to the one obtained in the MSSM.

A. One-loop effective potential

The finite temperature effective potential for the real Higgs scalars is

$$V(\varphi_i,T)=V_0(\varphi_i)+V_1(\varphi_i,T)+V_{daisy}(\varphi_i,T)+\cdots \tag{32}$$

where V_n is the n-loop contribution, and the additional term, V_{daisy}, will be discussed below. Also, φ_i, $i=1,2,s$ are the classical field variables corresponding to H_1^0, H_2^0, and S. ($\varphi_i=v_i$ at the T=0 minimum.) The tree-level part is

$$\begin{aligned}V_0(\varphi_i)=&m_1^2\varphi_1^2+m_2^2\varphi_2^2+m_s^2\varphi_s^2+2m_{12}^2\varphi_1\varphi_2+2t_s\varphi_s\\&+2a_\lambda\varphi_s\varphi_1\varphi_2+\frac{\overline{g^2}}{8}(\varphi_1^2-\varphi_2^2)^2+\lambda^2\varphi_s^2(\varphi_1^2+\varphi_2^2)\\&+\lambda^2\varphi_1^2\varphi_2^2.\end{aligned} \tag{33}$$

Note the cubic term, $a_\lambda\varphi_s\varphi_1\varphi_2$, which has no counterpart in the MSSM. In the $\overline{DR}$ scheme, the one-loop contribution reads

$$V_1(\varphi_i,T)=\sum_b g_b f_B(m_b^2,T)+\sum_f g_f f_F(m_f^2,T), \tag{34}$$

where b runs over bosons, f runs over Weyl fermions, and g_i is the number of (on-shell) degrees of freedom. To a very good approximation, the functions f_B, f_F are given by [39]

$$f_B(m^2,T)=\begin{cases}-\dfrac{\pi^2}{90}T^4+\dfrac{1}{24}m^2T^2-\dfrac{1}{12\pi}(m^2)^{3/2}T-\dfrac{m^4}{64\pi^2}\ln\left(\dfrac{Q^2}{\tilde{a}_BT^2}\right), & m/T\lesssim 2.2,\\ \dfrac{m^4}{64\pi^2}\left[\ln\left(\dfrac{m^2}{Q^2}\right)-\dfrac{3}{2}\right]-\left(\dfrac{m}{2\pi T}\right)^{3/2}T^4e^{-m/T}\left(1+\dfrac{15}{8}T/m+\cdots\right), & m/T\gtrsim 2.2,\end{cases} \tag{35}$$

$$f_F(m^2,T)=\begin{cases}-\dfrac{7\pi^2}{720}T^4+\dfrac{1}{48}m^2T^2+\dfrac{m^4}{64\pi^2}\ln\left(\dfrac{Q^2}{\tilde{a}_FT^2}\right), & m/T\lesssim 1.9,\\ -\dfrac{m^4}{64\pi^2}\left[\ln\left(\dfrac{m^2}{Q^2}\right)-\dfrac{3}{2}\right]-\left(\dfrac{m}{2\pi T}\right)^{3/2}T^4e^{-m/T}\left(1+\dfrac{15}{8}T/m+\cdots\right), & m/T\gtrsim 1.9.\end{cases}$$

Here, $\tilde{a}_B=(4\pi e^{-\gamma_E})^2$, $\tilde{a}_F=(\pi e^{-\gamma_E})^2$, m^2 is the field-dependent mass at zero temperature. We neglect V_2 and terms of higher order.

The third contribution to the potential, V_{daisy}, is a finite-temperature effect [40]. At zero temperature, one-loop boson self-energy diagrams which are quadratically divergent in the UV also develop an IR divergence as the boson mass is taken to zero. At finite-temperature, when $m\ll T$ the would-be IR divergence is cut off by T rather than m leading to a thermal contribution to the effective mass, $m^2\to\overline{m^2}=m^2+\alpha T^2$. Resumming the leading thermal contributions to bosonic self-energies modifies the effective potential by the amount

$$V_{daisy}=-\frac{1}{12\pi}\sum_b g_b(\overline{m_b^2}-m_b^2)^{3/2}, \tag{36}$$

where $\overline{m_b^2}$ is the thermal mass. The sum includes gauge bosons, although only the longitudinal modes of these develop a thermal contribution to their mass at leading order. The field-dependent mass matrices relevant to our analysis (including thermal corrections) are listed in Appendix A.

B. Tree-level analysis

To better understand the effect of the new cubic term, we have examined a simplified form of the potential which allows us to obtain analytic expressions for the critical temperature, T_c, and the field VEV's. If the cubic term plays a dominant role in making the electroweak phase transition first order, we expect this analysis to give a good qualitative description of the transition.

Our first simplifying assumption is that the ratio of the field values at the broken phase minimum remains constant up to T_c. That is, we fix $\tan\beta$, and consider variations in $\varphi=\sqrt{\varphi_1^2+\varphi_2^2}$. To make the one-loop part of the potential more manageable, we keep only the leading φ^2T^2 terms in the low-temperature expansion, and include only the contributions of the gauge bosons and the top. Since the stops are assumed to be heavy, the leading temperature-dependent contribution comes from the top provided λ lies below the perturbative bound, $\lambda\lesssim 0.8$. For larger values of λ the contributions from the Higgs bosons, charginos, and neutralinos become important. We shall restrict ourselves to the perturbative regime in the present analysis.

In terms of φ, φ_s, and β, the effective potential becomes $V=V_0+V_1$. The tree-level part is

$$V_0=M^2\varphi^2+m_s^2\varphi_s^2+2t_s\varphi_s+2\tilde{a}\varphi^2\varphi_s+\lambda^2\varphi^2\varphi_s^2+\tilde{\lambda}^2\varphi^4, \tag{37}$$

where we have defined

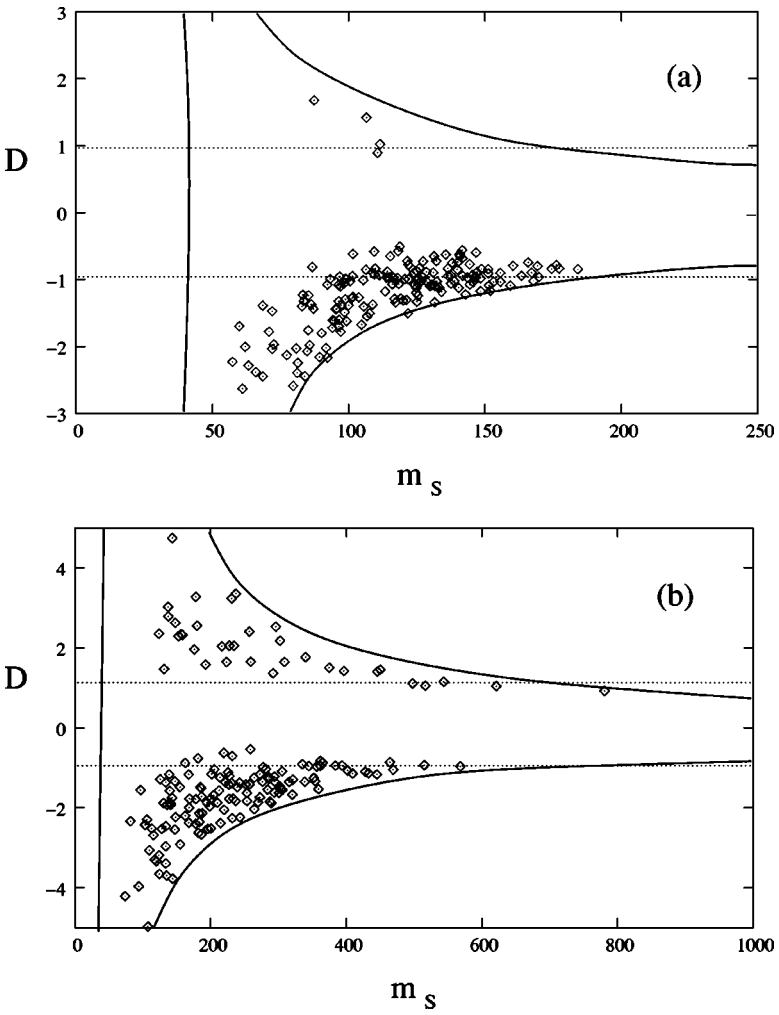

FIG. 4. Values of D for parameter sets leading to a strongly first order phase transition for: (a) λ below the perturbative bound; (b) general values of λ in the range $0.7<\lambda<2.0$. The region consistent with the experimental constraints lies within the area enclosed by the solid lines.

$$M^2 = m_1^2\cos^2\beta + m_2^2\sin^2\beta + m_{12}^2\sin 2\beta,$$

$$\tilde{a} = a_\lambda \sin\beta\cos\beta,$$

$$\tilde{\lambda}^2 = \frac{\lambda^2}{4}\sin^2 2\beta + \frac{\overline{g^2}}{8}\cos^2 2\beta. \tag{38}$$

Within our approximation, the one-loop part is

$$V_1 = \frac{1}{8}\left(g^2 + \frac{\overline{g^2}}{2} + 2y_t^2\sin^2\beta\right)\varphi^2 T^2. \tag{39}$$

To find the minimization conditions, we shall make use of the simple (quadratic) φ_s dependence and consider only the field-space trajectory $\partial V/\partial\varphi_s = 0$ along which the minimum of the potential is found. This condition allows us to eliminate φ_s in terms of φ giving

$$\varphi_s = -\left(\frac{t_s + \tilde{a}\varphi^2}{m_s^2 + \lambda^2\varphi^2}\right). \tag{40}$$

Inserting this back into the effective potential, we find

$$V(\varphi, T) = m^2(T)\varphi^2 - \frac{(t_s + \tilde{a}\varphi^2)^2}{m_s^2 + \lambda^2\varphi^2} + \tilde{\lambda}^2\varphi^4, \tag{41}$$

where $m^2(T) = M^2 + \frac{1}{8}(g^2 + \overline{g^2}/2 + 2y_t^2\sin^2\beta)T^2$.

The critical temperature, T_c, and the VEV at T_c, φ_c, are defined by the two conditions

$$V(\varphi_c, T_c) = V(\varphi = 0, T_c), \tag{42}$$

$$\left.\frac{\partial V}{\partial\varphi}\right|_{\varphi=\varphi_c} = 0.$$

Solving for φ_c and T_c we find

$$\varphi_c^2 = \frac{1}{\lambda^2}\left(-m_s^2 + \frac{1}{\tilde{\lambda}}\left|m_s\tilde{a} - \frac{\lambda^2 t_s}{m_s}\right|\right),$$

$$T_c^2 = 8(F(\varphi_c^2) - F(v^2)) \Big/ \left(g^2 + \frac{\overline{g^2}}{2} + 2y_t^2\sin^2\beta\right), \tag{43}$$

where

TABLE III. Sample parameter sets exhibiting a strongly first order electroweak phase transition.

Set	$\tan\beta$	λ	v_s (GeV)	a_λ (GeV)	$t_s^{1/3}$ (GeV)	M_a (GeV)	$\lvert M_2\rvert$ (GeV)	ϕ	φ_c (GeV)	T_c (GeV)	Ωh^2
A	1.70	0.619	−384	373	157	923	245	0.14	120	125	0.102
B	1.99	0.676	−220	305	143	914	418	2.57	145	95	0.010
C	1.10	0.920	−276	386	140	514	462	2.38	145	130	0.104

$$F(\varphi^2)=2\tilde{a}\left(\frac{t_s+\tilde{a}\varphi^2}{m_s^2+\lambda^2\varphi^2}\right)-\lambda^2\left(\frac{t_s+\tilde{a}\varphi^2}{m_s^2+\lambda^2\varphi^2}\right)^2-2\tilde{\lambda}^2\varphi^2. \tag{44}$$

Both φ_c^2 and T_c^2 must of course be positive if a solution is to exist. For $\varphi_c^2>0$, we need

$$m_s^2<\frac{1}{\tilde{\lambda}}\left|\frac{\lambda^2 t_s}{m_s}-m_s\tilde{a}\right|. \tag{45}$$

The positivity of T_c^2 requires that $F(\varphi_c^2)>F(v^2)$. Since increasing the temperature tends to decrease the field VEV, this condition will be satisfied if $F(\varphi^2)$ is a decreasing function which is the case provided

$$\left(m_s\tilde{a}-\frac{\lambda^2 t_s}{m_s}\right)^2<\tilde{\lambda}^2(m_s^2+\lambda^2\varphi^2)^3. \tag{46}$$

It is sufficient to demand that this hold for $\varphi=\varphi_c$, which gives

$$m_s^3(m_s^2\tilde{a}-\lambda^2 t_s)^2<\frac{1}{\tilde{\lambda}}|m_s^2\tilde{a}-\lambda^2 t_s|^3. \tag{47}$$

This is equivalent to the inequality in Eq. (45). Thus, Eq. (45) is the necessary condition for a first order phase transition. To satisfy this equation, m_s^2 must not be too large. This can be also seen from Eq. (41), which has only positive quadratic and quartic terms in the limit $\lambda^2\varphi^2\ll m_s^2$.

C. Numerical analysis

The results of the previous section have been examined more carefully by means of a numerical investigation of the one-loop effective potential. In this analysis, we consider only the dominant contributions which are those of the top, the stops, the gauge bosons, the Higgs bosons, the charginos, and the neutralinos. The corresponding field-dependent mass matrices, both at zero and finite temperature, are listed in Appendix A. For the purpose of calculating thermal masses, we assume that the remaining sfermions and the gluino are heavy enough to be neglected. We find that a strongly first order electroweak phase transition is possible within the nMSSM.

The procedure we use goes as follows: To begin, we specify the values of $(\beta, v_s, a_\lambda, t_s, M_a, \lambda, |M_2|, \phi)$, where $M_2=|M_2|e^{i\phi}$ is the complex W-ino soft mass. These are chosen randomly from the initial ranges listed in Table II. As above, the B-ino mass is taken to be $M_1=M_2/2$, and we fix the soft stop parameters to be $m_{Q_3}^2=m_{U_3}^2=(500\ \text{GeV})^2$, $a_t=100$ GeV. The subtraction scale is set at $Q^2=(150\ \text{GeV})^2$. For each parameter set we calculate the mass spectrum at zero temperature and impose the experimental constraints described in Sec. III. At this point we do not impose any dark matter constraint other than the necessary condition $m_{\tilde{N}_1}>25$ GeV. Since, for some parameter sets, the one-loop correction can destabilize the potential in the φ_s direction, we also check that the minimum at $(\varphi_1,\varphi_2,\varphi_s)=(v_1,v_2,v_s)$ is a global minimum at $T=0$. Finally, we calculate φ_c and T_c using the full potential, where T_c is taken to be the temperature at which the symmetric and broken phase minima are equal in depth, and $\varphi_c=\sqrt{\varphi_1^2+\varphi_2^2}$ is the broken phase VEV at this temperature.

In this way we have found several parameter sets which satisfy all the constraints listed above, and give $\varphi_c/T_c>0.9$, which we take as our criterion for a strongly first order transition [35,41].[3] Let us define

$$D=\frac{1}{\tilde{\lambda}m_s^2}\left(\frac{\lambda^2 t_s}{m_s}-\tilde{a}m_s\right) \tag{48}$$

where $m_s^2=-a_\lambda v_1 v_2/v_s-t_s/v_s-\lambda^2 v^2$ [see Eq. (10)], and $\tilde{a}$ and $\tilde{\lambda}$ are defined in Eq. (38). D is crucial in determining whether or not a first order phase transition occurs. The simplified analysis of Sec. IV B, Eq. (45) in particular, suggests that $|D|>1$ is a necessary condition for a first order transition. Figure 4 shows D plotted against m_s for both λ below the perturbative bound, and for general values in the range $0.7<\lambda<2.0$. The region surrounded by the solid lines in this figure corresponds to parameter sets consistent with the experimental constraints. This figure shows that among the parameter sets for which a strongly first order phase transition occurs, most satisfy $|D|>1$. On the other hand, we also find parameter sets with $|D|>1$ that do not exhibit a strongly first order phase transition, so this condition is not a sufficient one. The low m_s region in these plots is excluded since the potential tends to become unstable in the singlet direction for small values of this quantity. This leads to the additional requirement of $m_s^2\gtrsim(50\ \text{GeV})^2$.

The critical temperature for the phase transition generally falls in the range $T_c=100$–150 GeV. Table III shows the parameter values and transition temperatures for three of the

[3]This corresponds to $\varphi_c/T_c>1.3$ for φ normalized to 246 GeV.

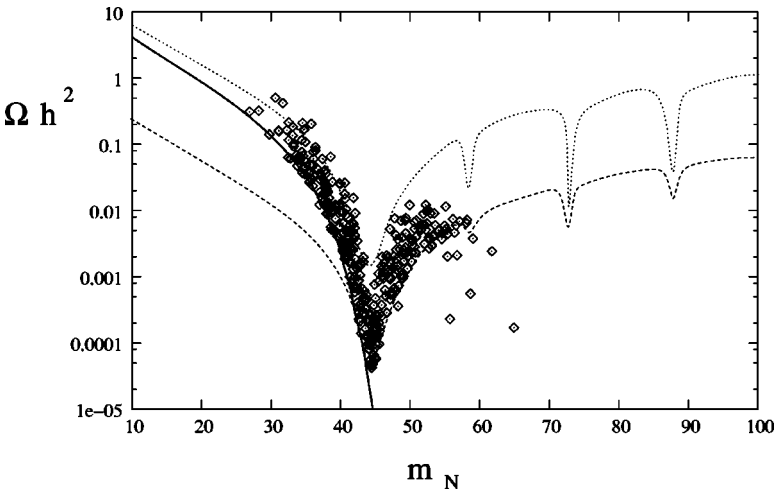

FIG. 5. Neutralino relic density as a function of mass for two values of the mixing parameter, $||N_{13}|^2-|N_{14}|^2|=0.1$ (dotted), 0.5 (dashed) and typical values of the Higgs mixing parameters. The region to the right of the thick solid line is consistent with the observed Z width. The scattered points correspond to parameter sets that give a strongly first order phase transition, and are consistent with perturbative unification.

successful parameter sets. The particle spectra corresponding to these are listed in Appendix C. Parameter sets *A* and *B*, with $|D|\simeq 1$, both satisfy the perturbative bound while *C*, for which $D\simeq 6.7$, exceeds it.

Sets *A* and *B* are typical of the (perturbative) parameter sets that give a strong phase transition. As we found in Sec. III A, the constraints in the chargino-neutralino sector, along with perturbative consistency, force $\lambda\sim 0.5$–0.8, $\tan\beta\sim 1.5$–5, and $|v_s|\sim 150$–500 GeV. For a given v_s, the values of a_λ and t_s must then be adjusted so that $m_s^2\gtrsim(50\ \mathrm{GeV})^2$ (Eq. (10)) and $|D|\gtrsim 1$ [Eq. (48)] if the potential is to be stable and the transition is to be strongly first order. These quantities are further constrained by the Higgs sector. We find that these requirements may be satisfied for $a_\lambda\sim 300$–600 GeV and $t_s\sim(50$–$200\ \mathrm{GeV})^3$. An upper bound on the value of m_s is obtained, that is about 200 GeV. This bound arises from the phenomenological constraints and, most importantly, due to the dependence of the parameter D on m_s, Eq. (48), from the condition $|D|\gtrsim 1$. This bound on m_s has important consequences for Higgs physics, as we will describe in Sec. VI.

The value of M_a, instead, does not appear to have much effect on the phase transition, but tends to be fairly large, $M_a\gtrsim 400$ GeV, due to the Higgs boson mass constraints. While large values of M_a help to increase the masses of the lightest Higgs states, they also tend to make EWBG less efficient [36–38]. Even so, EWBG is still able to account for the baryon asymmetry provided $\tan\beta\lesssim 2$, as we tend to find here [36].

V. NEUTRALINO DARK MATTER

As discussed above, the LSP in this model (for λ below the perturbative bound) is always the lightest neutralino, $\tilde{N}_1$, with a mass below about 60 GeV and a sizeable singlino component. This can be dangerous since a light, stable particle with very weak gauge couplings may produce a relic density much larger than is consistent with the observed cosmology. On the other hand, if the $\tilde{N}_1$ is able to annihilate sufficiently well, this state makes a good dark matter candidate [42].

For values of $\tan\beta$ and λ consistent with the perturbative limit, the LSP tends to be mostly singlino, but has a sizeable Higgsino component. Since $m_{\tilde{N}_1}\lesssim 60$ GeV, s-channel Z^0 exchange is the dominant annihilation mode. There are also contributions from s-channel *CP*-even and *CP*-odd Higgs boson exchanges generated by the $\lambda S H_1\cdot H_2$ term in the superpotential, although these tend to be very small except near the corresponding mass poles. Since we have assumed that

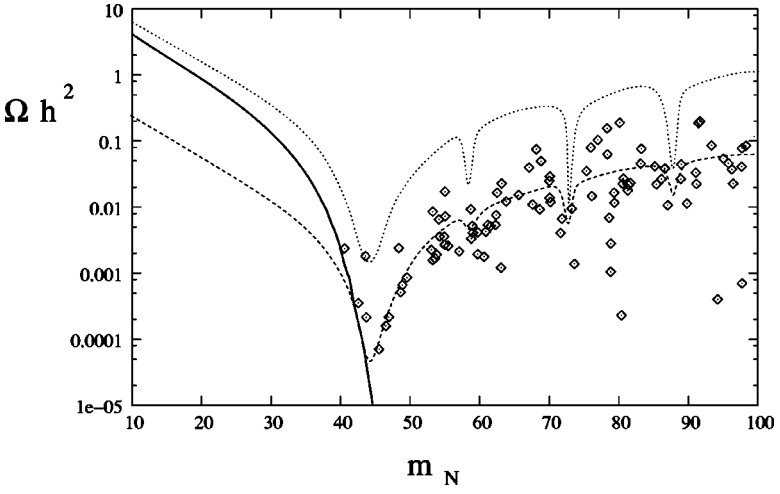

FIG. 6. Neutralino relic density as a function of mass for two values of the mixing parameter, $||N_{13}|^2-|N_{14}|^2|=0.1$ (dotted), 0.5 (dashed) and typical values of the Higgs mixing parameters. The region to the right of the thick solid line is consistent with the observed Z width. The scattered points correspond to parameter sets which give a strongly first order phase transition with $0.7<\lambda<1.2$.

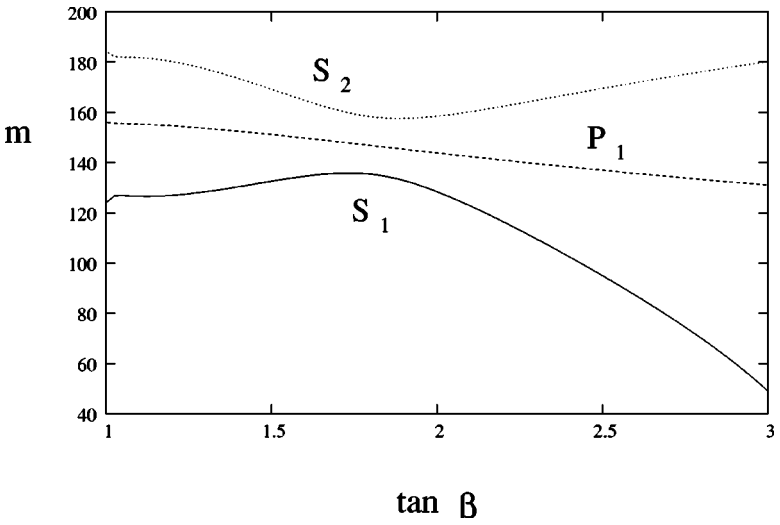

FIG. 7. Mass of the light Higgs bosons for typical parameter values consistent with EWBG.

all sfermions are heavy, we consider only these two channels in our analysis. The relevant couplings are listed in Appendix B. (The matrix element for s-channel Z-exchange is given in [43].) Let us stress that coannihilation between the lightest neutralino and the other chargino and neutralino states is not important, since for the parameter sets consistent with EWBG and the perturbative bound, the NLSP is always at least 15% (and almost always more than 25%) heavier than the LSP, implying that the coannihilation contribution is Boltzmann-suppressed.

The LSP mass range of interest lies near the Z-pole making the annihilation cross section a rapidly varying function of the mass. Since this can cause problems for the nonrelativistic expansion commonly used to calculate the thermal average of the cross section [44], we have instead followed the methods described in [45] to do the thermal average. This gives

$$\langle \sigma v \rangle = \int_{4M^2}^{\infty} ds \sqrt{s-4M^2} W K_1(\sqrt{s}/T)/16M^4 T K_2(M/T), \tag{49}$$

where $M = m_{\tilde{N}_1}$ is the neutralino mass, T is the temperature, s is the usual Mandelstam parameter, K_1 and K_2 are modified Bessel functions, and the quantity W is defined to be

$$W = \int \left[\prod_f \frac{d^3 p_f}{(2\pi)^3 2E_f} \right] (2\pi)^4 \delta^{(4)}\left(p_1 + p_2 - \sum_f p_f \right) |\mathcal{M}|^2, \tag{50}$$

where $|\mathcal{M}|^2$ is the squared matrix element averaged over initial states, and summed over final states.

To find the relic density we have solved the corresponding Boltzmann equation using the approximation method described in [46]. The ratio of mass to freeze out temperature, $x_f = M/T_f$, is given by the solution to

$$x_f = \ln\left[\frac{0.038(g/g_{*S}^{1/2}) M M_{Pl} \langle \sigma v \rangle(x_f)}{x_f^{1/2}} \right], \tag{51}$$

where $g = 2$ is the number of degrees of freedom of the neutralino, g_{*_S} is the total number of relativistic degrees of freedom at temperature T_f (we use a simple step approximation for both g_* and g_{*_S}), and M_{Pl} is the Planck mass. The relic density is then given by

$$\Omega h^2 = \frac{(1.07 \times 10^9 \ \text{GeV}^{-1})}{M_{Pl}} \left(\int_{x_f}^{\infty} dx \frac{\langle \sigma v \rangle(x)}{x^2} g_*^{1/2} \right)^{-1}. \tag{52}$$

Figures 5 and 6 show the relic densities obtained for parameter sets that satisfy the abovementioned experimental constraints, and are consistent with EWBG. A relic density consistent with the observed dark matter is obtained for neutralino masses in the range $m_{\tilde{N}_1} \simeq 30$–$40$ GeV. For neutralino masses greater than this, it appears to be difficult to generate a sufficiently large relic density to account for the dark matter. If we allow λ to exceed the perturbativity bound, a realistic dark matter candidate may be obtained for neutralino masses above about 65 GeV.

VI. PHENOMENOLOGICAL DISCUSSION

The region of parameter space consistent with EWBG, neutralino dark matter, and the experimental bounds is quite constrained, and leads to an interesting phenomenology. We shall focus on values of $\tan\beta$ and λ that satisfy the perturbativity bound.

The dark matter condition implies that the LSP of the model is the lightest neutralino with a mass in the range $m_{\tilde{N}_1} \simeq 30$–$40$ GeV, and is mostly singlino. For smaller values of $|M_2|$, the next-to-lightest neutralino is predominantly bino. Otherwise it is a mostly Higgsino state. In both cases, there are always two mostly Higgsino states with masses of order $|\lambda v_s| \lesssim 350$ GeV. The bound on the Higgsino masses comes from the bound on $|\mu|$ found in Sec. III A. This bound also implies that the lightest chargino state has a mass below this value.

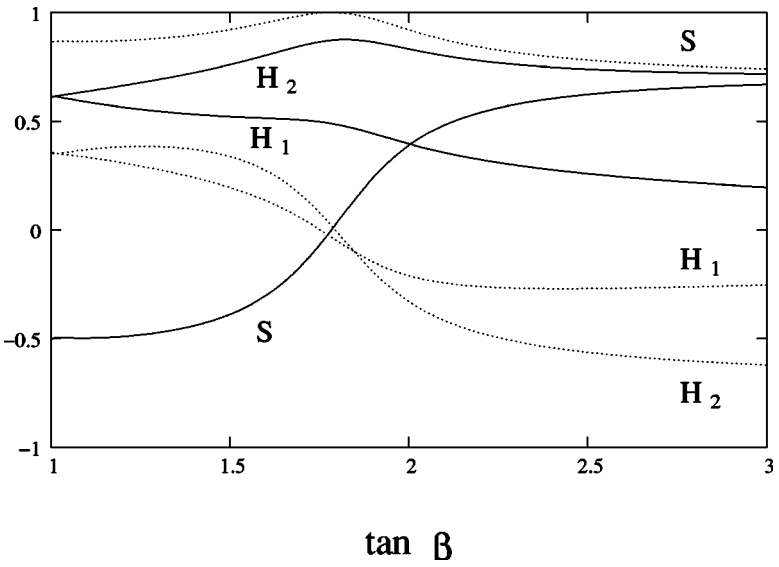

FIG. 8. Composition of the two light *CP*-even Higgs bosons for typical parameter values consistent with EWBG. The solid lines correspond to the components of S_1, $\mathcal{O}_{1i}^S$, while the dotted lines are those of S_2, $\mathcal{O}_{2i}^S$, for $i=1,2,S$. The composition of the P_1 state is not shown because it is almost pure singlet.

In the Higgs sector, since M_a tends to be fairly large, one *CP*-even Higgs state, one *CP*-odd Higgs state, and the charged Higgs end up with large masses of order M_a. The remaining *CP*-odd state is relatively light, and is nearly a pure singlet. For $M_a \to \infty$, the tree-level mass of this state goes to [see Eq. (24)]

$$m_P \to \sqrt{-(t_s + a_\lambda v^2 s_\beta c_\beta)/v_s} = \sqrt{m_s^2 + \lambda^2 v^2}, \tag{53}$$

which is less than 250 GeV for the values of t_s, v_s, and a_λ consistent with EWBG, as may be seen from Fig. 4.

The remaining two *CP*-even states also tend to be fairly light. In the $M_a \to \infty$ limit, the effective tree-level mass matrix for these states becomes

$$M_{S_{1,2}}^2 = \begin{pmatrix} M_Z^2 \cos^2 2\beta + \lambda^2 v^2 \sin^2 2\beta & v(a_\lambda \sin 2\beta + 2\lambda^2 v_s) \\ v(a_\lambda \sin 2\beta + 2\lambda^2 v_s) & -(t_s + a_\lambda v^2 s_\beta c_\beta)/v_s \end{pmatrix}. \tag{54}$$

Among the parameter ranges consistent with EWBG, the off-diagonal element of this matrix can be of the same order as the diagonal elements which leads to a strong mixing between the gauge eigenstates. However, too much mixing can produce an unacceptably light mass eigenstate, in conflict with the LEP bounds [33,34]. To avoid this, the two terms in the off-diagonal matrix element must cancel to some extent. If $a_\lambda = -2\lambda^2 v_s / \sin 2\beta$, the cancellation is exact, and the mixing goes to zero. The mass eigenstates then consist of the SM-Higgs-like linear combination $(\cos\beta H_1^0 + \sin\beta H_2^0)$ with a tree-level mass below 115 GeV, and a singlet state that is degenerate with the lightest *CP*-odd state. In general these states do mix, but since the mixing is limited by the Higgs boson mass constraint, one state remains predominantly SM-like while the other is mostly singlet. For finite M_a, the corrections to this picture are of order $a_\lambda v^2 / M_a^2$.

The mass of the SM-like *CP*-even state is increased significantly by the one-loop corrections from the top and the stops. For $m_Q^2 = m_U^2 = 500$ GeV, $a_t = 100$ GeV, as used in our analysis, we find that the mass of the lightest Higgs boson can be as large as 130 GeV, and still be consistent with EWBG.[4] This is somewhat larger than the corresponding MSSM limit of about 120 GeV [8], and is the result of the additional terms in the tree-level potential. These lead to a larger Higgs quartic coupling than in the MSSM, which sets the scale of the lightest SM-like *CP*-even state, while still allowing for a strongly first order electroweak phase transition.

Figures 7 and 8 show the mass and composition of the three light Higgs states (including the one-loop contributions from the top and the stops) for the representative parameter values $M_a = 900$ GeV, $t_s = (150\ \text{GeV})^3$, $v_s = -300$ GeV, $a_\lambda = 350$ GeV, and $\lambda = 0.7$. These values are typical of those consistent with the constraints and EWBG. The maximum of the mass of the lightest *CP*-even state occurs when the off-diagonal term in Eq. (54) vanishes; $\sin 2\beta = -2\lambda^2 v_s / a_\lambda$. The splitting between the P_1 and S_2 states at this point is due to the finite value of M_a. As $\tan\beta$ varies away from the maximum point, the mixing between the *CP*-even Higgs boson states increases and, for the specific parameters chosen in

[4]We do not expect two-loop corrections to significantly alter this result for the set of stop parameters used here.

Fig. 7, values of $\tan\beta \gtrsim 2.5$ are excluded by the current Higgs boson mass bounds obtained by the LEP experiments [33,34].

The discovery of these light states is more challenging than the MSSM case for two reasons. First, all three can have sizeable singlet components which reduce their couplings to the gauge bosons and quarks, and therefore their production cross sections. Second, these states can decay invisibly into pairs of the neutralino LSP. For *CP*-even Higgs boson masses below the weak gauge boson production threshold this mode dominates the decay width: $BR(S\to\tilde{N}_1\tilde{N}_1) \simeq 0.60$–$0.95$ for the SM-like state; $BR(S\to\tilde{N}_1\tilde{N}_1)\simeq 1$ for the mostly singlet state. However, for masses above (or near) the threshold, weak gauge boson final states become dominant unless the Higgs boson is a nearly pure singlet state.

Previous studies indicate that the most promising discovery mode for an invisibly decaying *CP*-even Higgs boson at the LHC is vector boson fusion (VBF) [47–50]. In Ref. [49] the authors find that, from the invisible modes alone, Higgs boson masses up to 150 GeV can be excluded at 95% C.L. with 10 fb^{-1} of integrated luminosity provided $\eta \gtrsim 0.35$, where

$$\eta = BR(h\to \mathrm{inv})\,\frac{\sigma(VBF)}{\sigma(VBF)_{SM}}. \tag{55}$$

If we treat these limits as being due only to statistical uncertainty and rescale them by luminosity, we obtain

$$\mathcal{L}_{95\%} \simeq \frac{1.2\ \mathrm{fb}^{-1}}{\eta^2}, \quad \mathcal{L}_{5\sigma} \simeq \frac{8.0\ \mathrm{fb}^{-1}}{\eta^2}, \tag{56}$$

where $\mathcal{L}_{95\%}$ and $\mathcal{L}_{5\sigma}$ are the luminosities needed for a 95% C.L. exclusion and a 5σ discovery respectively. For the SM-like *CP*-even state, we find $\eta \simeq 0.5$–0.9 among the parameter sets consistent with EWBG. This implies that, from the invisible channels alone, less than about 5 fb^{-1} of integrated luminosity is needed to exclude this state at 95% C.L., while 10–30 fb^{-1} is sufficient for a 5σ discovery. Similarly, we find $\eta \simeq 0$–0.35 for the mostly singlet *CP*-even state if the mass lies below the gauge boson threshold. Thus, at least 10 fb^{-1} is needed for a 95% C.L. exclusion and 65 fb^{-1} for a 5σ discovery using the invisible modes. On the other hand, if this state has a mass above the gauge boson threshold, the Higgs component is usually large enough that gauge boson final states completely dominate the branching ratio. Lastly, the light *CP*-odd state is nearly pure singlet and tends to decay invisibly, making it extremely difficult to observe.

VII. CONCLUSIONS

The origin of the matter-antimatter asymmetry and the source of the dark matter are two of the most important questions at the interface of particle physics and cosmology. In this article, we have investigated these questions within a next-to-minimal supersymmetric extension of the standard model. The nMSSM model, which elegantly solves the μ problem by adding a gauge singlet superfield, appears to be consistent with all current experimental constraints, does not suffer from the usual domain wall problem of the NMSSM, and leads to the stability of the proton and a neutralino LSP over cosmological times.

We have shown that a strongly first order electroweak phase transition, necessary to preserve the baryon asymmetry produced by electroweak baryogenesis, may be naturally obtained within this model. The strength of the phase transition is largely determined by terms in the tree-level nMSSM scalar potential. This differs from the MSSM, in which one-loop corrections from a light stop are needed to make the transition first order.

We have also shown that, if perturbative consistency is required to hold up to the GUT scale, the LSP of the model (in the absence of a light gravitino) is always the lightest neutralino, and has a mass below about 60 GeV. This state provides a viable dark matter candidate for neutralino masses in the range 30–40 GeV. Furthermore, we find that it is possible to achieve simultaneously both a realistic neutralino relic density and a strongly first order phase transition.

In the region of parameters consistent with both requirements, there are always at least two light *CP*-even and one light *CP*-odd Higgs bosons. These can decay invisibly into neutralinos providing an interesting modification to the standard Higgs physics processes.

ACKNOWLEDGMENTS

We would like to thank Csaba Balázs, Marcela Carena, Géraldine Servant, Tim Tait, and Ishai Ben-Dov for useful discussions. Work at ANL is supported in part by the US DOE, Div. of HEP Contract W-31-109-ENG-38.

APPENDIX A: FIELD-DEPENDENT MASSES

In this section we collect the field and temperature dependent mass matrices for those particles relevant to the analysis in Sec. IV. The leading thermal mass corrections were calculated following [51] for vanishing background field values; $\varphi_1=\varphi_2=\varphi_s=0$. Ignoring the singlet background is reasonable here since, in the parameter space of interest, the singlet VEV is closely related to the other Higgs VEV's. To leading order, only bosons receive thermal mass corrections. These come from quadratically divergent (at T=0) loops containing particles which are light compared to the temperature; $m \lesssim 2\pi T$ for bosons and $m \lesssim \pi T$ for fermions. For the purpose of calculating thermal masses we have taken the Higgs bosons, Higgsinos, electroweak gauginos, and the SM particles to be light, while treating the rest of the particles in the spectrum as heavy. We do not expect that a different choice of spectrum would change our phase transition results since the first order nature of the transition is determined by the tree-level potential rather than the cubic one-loop term in j_B.

1. Gauge bosons

At leading order, only the longitudinal components of the gauge bosons receive thermal corrections. The masses are

$$m_W^2=\frac{1}{2}g^2(\varphi_1^2+\varphi_2^2)+\Pi_{W^\pm},$$

$$\mathcal{M}_{Z\gamma}^2=\begin{pmatrix}\frac{1}{2}g^2(\varphi_1^2+\varphi_2^2)+\Pi_{W^3} & -\frac{1}{2}gg'(\varphi_1^2+\varphi_2^2)\\ -\frac{1}{2}gg'(\varphi_1^2+\varphi_2^2) & \frac{1}{2}g'^2(\varphi_1^2+\varphi_2^2)+\Pi_B\end{pmatrix}, \tag{A1}$$

where $\Pi_i=0$ for the transverse modes, and

$$\Pi_{W^\pm}=\frac{5}{2}g^2T^2,$$

$$\Pi_{W^3}=\frac{5}{2}g^2T^2,$$

$$\Pi_B=\frac{13}{6}g'^2T^2, \tag{A2}$$

for the longitudinal modes.

2. Tops and stops

$$m_t^2=y_t^2\varphi_2^2,$$

$$\mathcal{M}_{\tilde{t}}^2=\begin{pmatrix}m_Q^2+m_t^2+\frac{1}{4}\left(g^2-\frac{1}{3}g'^2\right)(\varphi_1^2-\varphi_2^2)+\Pi_{\tilde{t}_L} & a_t\varphi_2+\lambda\varphi_s\varphi_1\\ a_t\varphi_2+\lambda\varphi_s\varphi_1 & m_U^2+m_t^2+\frac{1}{3}g'^2(\varphi_1^2-\varphi_2^2)+\Pi_{\tilde{t}_R}\end{pmatrix}, \tag{A3}$$

where

$$\Pi_{\tilde{t}_L}=\frac{1}{3}g_s^2T^2+\frac{5}{16}g^2T^2+\frac{5}{432}g'^2T^2+\frac{1}{6}y_t^2T^2,$$

$$\Pi_{\tilde{t}_R}=\frac{1}{3}g_s^2T^2+\frac{5}{27}g'^2T^2+\frac{1}{3}y_t^2T^2. \tag{A4}$$

3. Higgs bosons

The *CP*-even mass matrix elements are

$$\mathcal{M}_{S_{11}}^2=m_1^2+\lambda^2(\varphi_2^2+\varphi_s^2)+\frac{\overline{g^2}}{4}(3\varphi_1^2-\varphi_2^2)+\Pi_{H_1},$$

$$\mathcal{M}_{S_{12}}^2=m_{12}^2+2\varphi_1\varphi_2\left(\lambda^2-\frac{\overline{g^2}}{4}\right)+a_\lambda\varphi_s,$$

$$\mathcal{M}_{S_{13}}^2=a_\lambda\varphi_2+2\lambda^2\varphi_1\varphi_s,$$

$$\mathcal{M}_{S_{22}}^2=m_2^2+\lambda^2(\varphi_1^2+\varphi_s^2)+\frac{\overline{g^2}}{4}(3\varphi_2^2-\varphi_1^2)+\Pi_{H_2}, \tag{A5}$$

$$\mathcal{M}_{S_{23}}^2=a_\lambda\varphi_1+2\lambda^2\varphi_2\varphi_s,$$

$$\mathcal{M}_{S_{33}}^2=m_s^2+\lambda^2(\varphi_1^2+\varphi_2^2)+\Pi_S,$$

where the leading thermal corrections are

$$\Pi_{H_1}=\frac{1}{8}g'^2T^2+\frac{3}{8}g^2T^2+\frac{1}{12}\lambda^2T^2,$$

$$\Pi_{H_2}=\frac{1}{8}g'^2T^2+\frac{3}{8}g^2T^2+\frac{1}{12}\lambda^2T^2+\frac{1}{4}y_t^2, \tag{A6}$$

$$\Pi_S=\frac{1}{6}\lambda^2T^2.$$

For the *CP*-odd states we have

$$\mathcal{M}_{P_{11}}^2=m_1^2+\lambda^2(\varphi_2^2+\varphi_s^2)-\frac{\overline{g^2}}{4}(\varphi_2^2-\varphi_1^2)+\Pi_{H_1},$$

$$\mathcal{M}_{P_{12}}^2=-m_{12}^2-a_\lambda\varphi_s,$$

$$\mathcal{M}_{P_{13}}^2=-a_\lambda\varphi_2,$$

$$\mathcal{M}_{P_{22}}^2=m_2^2+\lambda^2(\varphi_1^2+\varphi_s^2)+\frac{\overline{g^2}}{4}(\varphi_2^2-\varphi_1^2)+\Pi_{H_2}, \tag{A7}$$

$$\mathcal{M}_{P_{23}}^2=-a_\lambda\varphi_1,$$

$$\mathcal{M}_{P_{33}}^2=m_s^2+\lambda^2(\varphi_1^2+\varphi_2^2)+\Pi_S,$$

where the thermal corrections are as above.

The charged Higgs boson mass matrix is

$$\mathcal{M}^2_{H^\pm_{11}} = m_1^2 + \lambda^2\varphi_s^2 - \frac{\overline{g^2}}{4}(\varphi_2^2-\varphi_1^2) + \frac{g^2}{2}\varphi_2^2 + \Pi_{H_1},$$

$$\mathcal{M}^2_{H^\pm_{12}} = -\left(\lambda^2 - \frac{g^2}{2}\right)\varphi_1\varphi_2 - m_{12}^2 - a_\lambda\varphi_s, \tag{A8}$$

$$\mathcal{M}^2_{H^\pm_{22}} = m_2^2 + \lambda^2\varphi_s^2 + \frac{\overline{g^2}}{4}(\varphi_2^2-\varphi_1^2) + \frac{g^2}{2}\varphi_1^2 + \Pi_{H_2}.$$

4. Charginos and neutralinos

The chargino mass matrix reads

$$M_{\chi^\pm} = \begin{pmatrix} 0 & X^t \\ X & 0 \end{pmatrix} \tag{A9}$$

where

$$X = \begin{pmatrix} M_2 & g\varphi_2 \\ g\varphi_1 & -\lambda\varphi_s \end{pmatrix}. \tag{A10}$$

For the neutralinos we have

$$M_{\tilde{N}} = \begin{pmatrix} M_1 & \cdot & \cdot & \cdot & \cdot \\ 0 & M_2 & \cdot & \cdot & \cdot \\ -\frac{g'}{\sqrt{2}}\varphi_1 & \frac{g}{\sqrt{2}}\varphi_1 & 0 & \cdot & \cdot \\ \frac{g'}{\sqrt{2}}\varphi_2 & -\frac{g}{\sqrt{2}}\varphi_2 & \lambda\varphi_s & 0 & \cdot \\ 0 & 0 & \lambda\varphi_2 & \lambda\varphi_1 & 0 \end{pmatrix}. \tag{A11}$$

We have taken $M_1 = M_2/2$ and have allowed M_2 to be complex in our analysis.

APPENDIX B: HIGGS AND NEUTRALINO COUPLINGS

We list here the Higgs and neutralino couplings relevant to our analysis. All fermions are written in terms of four-component spinors to facilitate the derivation of the Feynman rules. As above, Eq. (18), we define the unitary matrix N_{ij} by

$$\tilde{N}_i = N_{ij}\psi_j^0 \tag{B1}$$

where $(\psi_i^0) = (\widetilde{B^0}, \widetilde{W^0}, \widetilde{H_1^0}, \widetilde{H_2^0}, \tilde{S})$. Similarly, as in Eq. (28) we define the orthogonal matrices $\mathcal{O}^S$ and $\mathcal{O}^P$ by

$$\begin{pmatrix} S_1 \\ S_2 \\ S_3 \end{pmatrix} = \mathcal{O}^S \begin{pmatrix} \phi_1 \\ \phi_2 \\ \phi_s \end{pmatrix}; \quad \begin{pmatrix} P_1 \\ P_2 \end{pmatrix} = \mathcal{O}^P \begin{pmatrix} A^0 \\ a_s \end{pmatrix}. \tag{B2}$$

1. Neutralino couplings

ZNN [1]:

$$\mathcal{L}_{ZNN} = \frac{g}{2\cos\theta_W} Z_\mu \bar{\tilde{N}}_i \gamma^\mu (\mathcal{O}^N_{ij} P_L - \mathcal{O}^{N^*}_{ij} P_R)\tilde{N}_j \tag{B3}$$

where

$$\mathcal{O}^N_{ij} = \frac{1}{2}(N_{i4}N^*_{j4} - N_{i3}N^*_{j3}). \tag{B4}$$

For the Higgs-neutralino couplings we consider only the contribution from the $\lambda S H_1 \cdot H_2$ term in the superpotential. We therefore neglect the contribution due to mixing with the gauginos.

SNN:

$$\mathcal{L}_{SNN} = -\frac{\lambda}{\sqrt{2}} S_k \bar{\tilde{N}}_i (\overline{A}^k_{ij} P_L + A^k_{ij} P_R)\tilde{N}_j, \tag{B5}$$

where

$$A^k_{ij} = \mathcal{O}^S_{k1} Q^{45}_{ij} + \mathcal{O}^S_{k2} Q^{35}_{ij} + \mathcal{O}^S_{k3} Q^{34}_{ij},$$

$$Q^{ab}_{ij} = \frac{1}{2}(N^*_{ia}N^*_{jb} + N^*_{ib}N^*_{ja}).$$

$\overline{A}^k_{ij}$ is related to A^k_{ij} by the replacement $N^*_{ij} \to N_{ij}$.

PNN:

$$\mathcal{L}_{PNN} = -i\frac{\lambda}{\sqrt{2}} S_k \bar{\tilde{N}}_i (\overline{B}^k_{ij} P_L - B^k_{ij} P_R)\tilde{N}_j, \tag{B6}$$

where

$$B^k_{ij} = s_\beta \mathcal{O}^P_{k1} Q^{45}_{ij} + c_\beta \mathcal{O}^P_{k1} Q^{35}_{ij} + \mathcal{O}^P_{k2} Q^{34}_{ij}.$$

As with A^k_{ij}, $\overline{B}^k_{ij}$ is related to B^k_{ij} by the replacement $N^*_{ij} \to N_{ij}$.

TABLE IV. Higgs scalar masses.

Set	S_1 (GeV)	S_2 (GeV)	S_3 (GeV)	P_1 (GeV)	P_2 (GeV)	$H^\pm$ (GeV)
A	115	158	925	135	927	922
B	116	182	914	164	917	911
C	121	219	504	115	534	498

TABLE V. Neutralino and chargino masses.

Set	$\tilde{N}_1$ (GeV)	$\tilde{N}_2$ (GeV)	$\tilde{N}_3$ (GeV)	$\tilde{N}_4$ (GeV)	$\tilde{N}_5$ (GeV)	$\chi_1^\pm$ (GeV)	$\chi_2^\pm$ (GeV)
A	33.3	107	181	278	324	165	320
B	52.4	168	203	221	432	151	432
C	77.1	228	268	331	474	257	474

TABLE VI. Composition of the lightest neutralino and Higgs state.

Set	$\lvert N_{11}\rvert$	$\lvert N_{12}\rvert$	$\lvert N_{13}\rvert$	$\lvert N_{14}\rvert$	$\lvert N_{15}\rvert$	$\mathcal{O}^S_{11}$	$\mathcal{O}^S_{12}$	$\mathcal{O}^S_{13}$	$\mathcal{O}^P_{11}$	$\mathcal{O}^P_{12}$
A	0.13	0.10	0.11	0.37	0.91	0.46	0.74	−0.50	0.08	0.99
B	0.07	0.07	0.16	0.52	0.84	0.42	0.80	−0.44	0.07	0.99
C	0.01	0.01	0.28	0.33	0.90	0.70	0.53	0.48	0.26	0.97

Finally we note that in converting these couplings into Feynman rules, one must insert an additional factor of two since the neutralinos are written as Majorana spinors [1].

2. Higgs couplings

The relevant couplings of the Higgs scalars to the gauge bosons are given in Sec. III B above. We list here the couplings of the Higgs boson to the third generation quarks.

$S\bar{f}f$:

$$\mathcal{L}_{S\bar{f}f} = -\frac{1}{\sqrt{2}} y_b \mathcal{O}^S_{k1} S_k \bar{b} b - \frac{1}{\sqrt{2}} y_t \mathcal{O}^S_{k2} S_k \bar{t} t. \tag{B7}$$

$P\bar{f}f$:

$$\mathcal{L}_{P\bar{f}f} = \frac{i}{\sqrt{2}} y_b s_\beta \mathcal{O}^P_{k1} P_k \bar{b} \gamma^5 b + \frac{i}{\sqrt{2}} y_t c_\beta \mathcal{O}^S_{k1} P_k \bar{t} \gamma^5 t. \tag{B8}$$

The couplings of the Higgs states to the other matter fermions follow the same pattern.

3. LSP lifetime

Having listed the Higgs-neutralino couplings, we may now present an estimate for the lifetime of the LSP in the $\mathbb{Z}_5^R$ symmetric scenario. This symmetry allows the $d=5$ operator $\hat{S}\hat{S}\hat{H}_2\hat{L}$ in the superpotential, which can lead to the decay of the neutralino LSP. This operator generates a coupling which allows the neutralino to decay into a neutrino and a pair of off-shell neutral Higgs scalars, or an electron, a neutral Higgs scalar, and a charged Higgs scalar. We shall focus on the first mode with intermediate neutral *CP*-even states and a mostly singlino LSP. This gives a more stringent constraint than the charged mode, and the analysis with intermediate neutral *CP*-odd states is analogous. We will also assume that each of the neutral Higgs bosons subsequently decays into $\bar{b}b$. With these assumptions, we find

$$\Gamma(\tilde{N}_1 \to \nu \bar{b} b \bar{b} b) \sim \frac{\pi}{2(4\pi^2)^4} \frac{y_b^4 |N^*_{15} \mathcal{O}^S_{i3} \mathcal{O}^S_{j2} \mathcal{O}^S_{1i} \mathcal{O}^S_{1j}|^2}{\Lambda^2 m_H^8} \left(\frac{m_{\tilde{N}}}{5}\right)^{11} \tag{B9}$$

where Λ is the cutoff scale, m_H is the Higgs boson mass in the intermediate propagators, and we have set all final state momenta to $m_{\tilde{N}}/5$. Setting the mixing factor to unity, taking $m_{\tilde{N}}/m_H \sim 1$ and $\tan\beta = 2$, and demanding that $\Gamma < H_0$, we find

$$\Lambda^2 \gtrsim \left(\frac{m_{\tilde{N}}}{\text{GeV}}\right)^3 10^{23}\ \text{GeV}^2 \tag{B10}$$

which translates into $\Lambda \gtrsim 3 \times 10^{14}$ GeV for $m_{\tilde{N}} = 100$ GeV.

APPENDIX C: SAMPLE MASS SPECTRA

We list in Table IV the Higgs boson mass spectra for the sample parameter sets A, B, and C listed in Table III. Table V shows the neutralino and chargino masses for these parameter sets, while Table VI displays the composition of the lightest neutralino, $\tilde{N}_1$, the lightest *CP*-even Higgs boson, S_1, and the lightest *CP*-odd Higgs boson, P_1.

[1] H.P. Nilles, Phys. Rep. **110**, 1 (1984); H.E. Haber and G.L. Kane, *ibid.* **117**, 75 (1985).

[2] S.P. Martin, hep-ph/9709356.

[3] C.T. Hill and E.H. Simmons, Phys. Rep. **381**, 235 (2003); **390**, 553(E) (2004).

[4] M. Fukugita and T. Yanagida, Phys. Lett. B **174**, 45 (1986).

[5] W. Buchmüller, P. Di Bari, and M. Plümacher, Nucl. Phys. **B665**, 445 (2003).

[6] A.G. Cohen, D.B. Kaplan, and A.E. Nelson, Annu. Rev. Nucl. Part. Sci. **43**, 27 (1993); M. Quirós, Helv. Phys. Acta **67**, 451 (1994); V.A. Rubakov and M.E. Shaposhnikov, Phys. Usp. **39**, 461 (1996); M. Carena and C.E.M. Wagner, hep-ph/9704347; A. Riotto and M. Trodden, Annu. Rev. Nucl. Part. Sci. **49**, 35 (1999); M. Quirós and M. Seco, Nucl. Phys. B (Proc. Suppl.) **81**, 63 (2000); L. Buvakovsky and T. Goldman, Phys. Rev. D **56**, 1368 (1997).

[7] M. Carena, M. Quirós, and C.E.M. Wagner, Phys. Lett. B **380**, 81 (1996); M. Laine, Nucl. Phys. **B481**, 43 (1996); M. Losada, Phys. Rev. D **56**, 2893 (1997); G. Farrar and M. Losada, Phys. Lett. B **406**, 60 (1997); B. de Carlos and J.R. Espinosa, Nucl. Phys. **B503**, 24 (1997); D. Bodeker, P. John, M. Laine, and M.G. Schmidt, *ibid.* **B497**, 387 (1997); M. Carena, M. Quirós, and C.E.M. Wagner, *ibid.* **B524**, 3 (1998); M. Laine and K. Rummukainen, *ibid.* **B535**, 423 (1998); M. Losada, *ibid.* **B537**, 3 (1999); **B569**, 125 (2000); M. Laine and M. Losada, *ibid.* **B582**, 277 (2000); M. Laine and K. Rummukainen, *ibid.* **B597**, 23 (2001).

[8] C. Balazs, M. Carena, and C.E.M. Wagner, hep-ph/0403224.

[9] See, for example, G.F. Giudice and A. Masiero, Phys. Lett. B **206**, 480 (1988).

[10] P. Fayet, Nucl. Phys. **B90**, 104 (1975); H.-P. Nilles, M. Srednicki, and D. Wyler, Phys. Lett. **120B**, 346 (1983); J.-M. Frere, D.R.T. Jones, and S. Raby, Nucl. Phys. **B222**, 11 (1983); J.-P. Derendinger and C.A. Savoy, *ibid.* **B237**, 307 (1984); B.R. Greene and P.J. Miron, Phys. Lett. **168B**, 226 (1986); J. Ellis, K. Enqvist, D.V. Nanopoulos, K.A. Olive, M. Quiros, and F. Zwirner, Phys. Lett. B **176**, 403 (1986); L. Durand and J.L. Lopez, *ibid.* **217**, 463 (1989); M. Drees, Int. J. Mod. Phys. A **4**, 3635 (1989); U. Ellwanger, Phys. Lett. B **303**, 271 (1993); U. Ellwanger, M. Rausch de Taubenberg, and C.A. Savoy, *ibid.* **315**, 331 (1993); Z. Phys. C **67**, 665 (1995); Nucl. Phys. **B492**, 21 (1997); P.N. Pandita, Phys. Lett. B **318**, 338 (1993); Z. Phys. C **59**, 575 (1993); T. Elliott, S.F. King, and P.L. White, Phys. Lett. B **305**, 71 (1993); **314**, 56 (1993); Phys. Rev. D **49**, 2435 (1994); Phys. Lett. B **351**, 213 (1995); K.S. Babu and S.M. Barr, Phys. Rev. D **49**, R2156 (1994); S.F. King and P.L. White, *ibid.* **52**, 4183 (1995); N. Haba, M. Matsuda, and M. Tanimoto, *ibid.* **54**, 6928 (1996); F. Franke and H. Fraas, Int. J. Mod. Phys. A **12**, 479 (1997); S.W. Ham, S.K. Oh, and H.S. Song, Phys. Rev. D **61**, 055010 (2000); D.A. Demir, E. Ma, and U. Sarkar, J. Phys. G **26**, L117 (2000); R.B. Nevzorov and M.A. Trusov, Phys. At. Nucl. **64**, 1299 (2001); U. Ellwanger and C. Hugonie, Eur. Phys. J. C **25**, 297 (2002); U. Ellwanger, J.F. Gunion, C. Hugonie, and S. Moretti, hep-ph/0305109; D.J. Miller and S. Moretti, hep-ph/0403137.

[11] S.A. Abel, S. Sarkar, and P.L. White, hep-ph/9507333.

[12] S.A. Abel, S. Sarkar, and P.L. White, Nucl. Phys. **B454**, 663 (1995).

[13] J. Bagger and E. Poppitz, Phys. Rev. Lett. **71**, 2380 (1993); J. Bagger, E. Poppitz, and L. Randall, Nucl. Phys. **B455**, 59 (1995); S.A. Abel, *ibid.* **B480**, 55 (1996).

[14] C. Panagiotakopoulos and K. Tamvakis, Phys. Lett. B **469**, 145 (1999); **446**, 224 (1999).

[15] C. Panagiotakopoulos and A. Pilaftsis, Phys. Rev. D **63**, 055003 (2001).

[16] A. Dedes, C. Hugonie, S. Moretti, and K. Tamvakis, Phys. Rev. D **63**, 055009 (2001).

[17] Y. Okada, M. Yamaguchi, and T. Yanagida, Prog. Theor. Phys. **85**, 1 (1991); M. Carena, M. Quiros, and C.E.M. Wagner, Nucl. Phys. **B461**, 407 (1996); H.E. Haber, R. Hempfling, and A.H. Hoang, Z. Phys. C **75**, 539 (1997); S. Heinemeyer, W. Hollik, and G. Weiglein, Phys. Rev. D **58**, 091701 (1998); Phys. Lett. B **440**, 296 (1998); Eur. Phys. J. C **9**, 343 (1999); J.R. Espinosa and R.J. Zhang, J. High Energy Phys. **03**, 026 (2000); Nucl. Phys. **B586**, 3 (2000); M. Carena, H.E. Haber, S. Heinemeyer, W. Hollik, C.E.M. Wagner, and G. Weiglein, *ibid.* **B580**, 29 (2000); G. Degrassi, P. Slavich, and F. Zwirner, *ibid.* **B611**, 403 (2001); A. Brignole, G. Degrassi, P. Slavich, and F. Zwirner, *ibid.* **B631**, 195 (2002); S.P. Martin, Phys. Rev. D **67**, 095012 (2003).

[18] M. Quiros, Nucl. Phys. B (Proc. Suppl.) **101**, 401 (2001).

[19] M. Pietroni, Nucl. Phys. **B402**, 27 (1993).

[20] A.T. Davies, C.D. Froggatt, and R.G. Moorhouse, Phys. Lett. B **372**, 88 (1996).

[21] S.J. Huber and M.G. Schmidt, Nucl. Phys. **B606**, 183 (2001).

[22] M. Bastero-Gil, C. Hugonie, S.F. King, D.P. Roy, and S. Vempati, Phys. Lett. B **489**, 359 (2000).

[23] J. Kang, P. Langacker, T.j. Li, and T. Liu, hep-ph/0402086.

[24] R. Harnik, G.D. Kribs, D.T. Larson, and H. Murayama, Phys. Rev. D **70**, 015002 (2004); R. Kitano, G.D. Kribs, and H. Murayama, *ibid.* **70**, 035001 (2004).

[25] J.R. Ellis, J.F. Gunion, H.E. Haber, L. Roszkowski, and F. Zwirner, Phys. Rev. D **39**, 844 (1989).

[26] J.C. Romao, Phys. Lett. B **173**, 309 (1986).

[27] OPAL Collaboration, G. Abbiendi *et al.*, Eur. Phys. J. C **35**, 1 (2004).

[28] LEP Collaborations, hep-ex/0101027.

[29] J.R. Espinosa and M. Quiros, Phys. Lett. B **279**, 92 (1992).

[30] See, for example, J.S. Lee, A. Pilaftsis, M. Carena, S.Y. Choi, M. Drees, J.R. Ellis, and C.E.M. Wagner, Comput. Phys. Commun. **156**, 283 (2004), and references therein.

[31] LEP Higgs Working Group for Higgs boson searches Collaboration, hep-ex/0107031.

[32] LEP Higgs Working Group Collaboration, hep-ex/0107030.

[33] ALEPH Collaboration, R. Barate *et al.*, Phys. Lett. B **565**, 61 (2003).

[34] LEP Higgs Working for Higgs boson searches Collaboration, hep-ex/0107032.

[35] M. Carena, M. Quiros, and C.E.M. Wagner, Phys. Lett. B **380**, 81 (1996).

[36] M. Carena, M. Quiros, M. Seco, and C.E.M. Wagner, Nucl. Phys. **B650**, 24 (2003).

[37] J.M. Cline, M. Joyce, and K. Kainulainen, J. High Energy Phys. **07**, 018 (2000).

[38] M. Carena, J.M. Moreno, M. Quiros, M. Seco, and C.E.M.

Wagner, Nucl. Phys. **B599**, 158 (2001).
[39] G.W. Anderson and L.J. Hall, Phys. Rev. D **45**, 2685 (1992).
[40] J. I. Kapusta, *Finite Temperature Field Theory* (Cambridge University Press, Cambridge, England, 1989); M.E. Carrington, Phys. Rev. D **45**, 2933 (1992); P. Arnold and O. Espinosa, *ibid.* **47**, 3546 (1993); **50**, 6662(E) (1994).
[41] A.G. Cohen, D.B. Kaplan, and A.E. Nelson, Annu. Rev. Nucl. Part. Sci. **43**, 27 (1993).
[42] K.A. Olive and D. Thomas, Nucl. Phys. **B355**, 192 (1991).
[43] K. Griest, Phys. Rev. D **38**, 2357 (1988); **39**, 3802(E) (1989).
[44] K. Griest and D. Seckel, Phys. Rev. D **43**, 3191 (1991).
[45] P. Gondolo and G. Gelmini, Nucl. Phys. **B360**, 145 (1991).
[46] E. W. Kolb and M. S. Turner, *The Early Universe* (Addison-Wesley, Redwood City, CA, 1990).
[47] J.F. Gunion, Phys. Rev. Lett. **72**, 199 (1994); D. Choudhury and D.P. Roy, Phys. Lett. B **322**, 368 (1994).
[48] O.J.P. Eboli and D. Zeppenfeld, Phys. Lett. B **495**, 147 (2000).
[49] D. Cavalli *et al.*, hep-ph/0203056.
[50] R.M. Godbole, M. Guchait, K. Mazumdar, S. Moretti, and D.P. Roy, Phys. Lett. B **571**, 184 (2003).
[51] A. Brignole, J.R. Espinosa, M. Quiros, and F. Zwirner, Phys. Lett. B **324**, 181 (1994); D. Comelli and J.R. Espinosa, Phys. Rev. D **55**, 6253 (1997).